# Diversity and distribution of cold-seep fauna associated with different geological and environmental settings at mud volcanoes and pockmarks of the Nile Deep-Sea Fan

Bénédicte Ritt, Catherine Pierre, Olivier Gauthier, F. Wenzhöfer, Antje Boetius, Jozée Sarrazin

# Diversity and distribution of cold-seep fauna associated with different geological and environmental settings at mud volcanoes and pockmarks of the Nile Deep-Sea Fan

Bénédicte Ritt[a, *], Catherine Pierre[b], Olivier Gauthier[a, c, d], Frank Wenzhöfer[e, f], Antje Boetius[e, f] and Jozée Sarrazin[a, *]

[a]Ifremer, Centre de Brest, Département Etude des Ecosystèmes Profonds/Laboratoire Environnement Profond, BP 70, 29280 Plouzané, France
[b]LOCEAN, UMR 7159, Université Pierre et Marie Curie,75005 Paris, France
[c]LEMAR, UMR 6539, Universiteé de Bretagne Occidentale, Place N. Copernic, 29200 Plouzaneé, France
[d]Ecole Pratique des Hautes Etudes CBAE, UMR 5059, 163 rue Auguste Broussonet, 34000 Montpellier, France
[e]MPI, Habitat Group, Celsiusstrasse 1, 28359 Bremen, Germany
[f]AWI, HGF MPG Research Group on Deep Sea Ecology and Technology, 27515 Bremerhaven, Germany

*: Corresponding authors : Bénédicte Ritt, email address : benedicte.ritt@ifremer.fr ; benedicte.ritt@temple.edu
Jozée Sarrazin, Tel.: +33 2 98 22 43 29, Fax: +33 2 98 22 47 57, email address :  jozee.sarrazin@ifremer.fr

**Abstract :**

The Nile Deep-Sea Fan (NDSF) is located on the passive continental margin off Egypt and is characterized by the occurrence of active fluid seepage such as brine lakes, pockmarks and mud volcanoes. This study characterizes the structure of faunal assemblages of such active seepage systems of the NDSF. Benthic communities associated with reduced, sulphidic microhabitats such as sediments and carbonate crusts were sampled by remotely operated vehicles during two cruises in 2006 (BIONIL) and 2007 (MEDECO). Environmental conditions and biological factors including family-level faunal composition, density and diversity were measured at local and regional scales. Significant differences were detected at different spatial scales: (1) the fauna of reduced habitats differed substantially in activity, diversity and biomass from the non-seep environment at similar water depth, (2) cold seep microhabitats showed differences in community structure and composition related to substratum type as well as to the intensity and location of fluid emissions.

1. Introduction

Since their discovery on the Florida Escarpment in the Gulf of Mexico (Paull et al. 1984), cold seeps have been reported along convergent plate boundaries on active as well as passive continental margins, where over-pressure in the sediments controls the emission of fluids enriched in methane or other hydrocarbons to the seafloor and hydrosphere (Milkov 2000; Dimitrov 2002). Depending on their geophysical settings, these cold seeps are associated with distinct geological features such as gas hydrates, pockmarks, brine lakes and mud volcanoes (MVs) (Milkov 2000; Hovland et al. 2002; Judd and Hovland 2007; Foucher et al. 2009). To date, hundreds of seep sites supporting chemosynthesis-based communities have been encountered throughout the world's oceans (Sibuet and Olu 1998; Levin 2005; Campbell 2006; Baker et al. 2010).

The Eastern Mediterranean Sea is one of the world's MV and pockmark hotspots (Kopf 2002; Foucher et al. 2009). Most of the MVs are associated with the active Mediterranean Ridge that stretches over more than 1500 km (Cita et al. 1981) and the thickly sedimented Nile Deep-Sea Fan (NDSF) along the Mesozoic-rifted continental margin of northern Egypt (Bellaiche et al. 2001; Mascle et al. 2001; Loncke et al. 2004; Mascle et al. 2006). The present study focuses on sites of the NDSF that have been explored since 2003 in the frame of the European Science Foundation (ESF) MEDIFLUX program (2003-2007) and the European 6th Framework Program project HERMES (2005-2009).

The NDSF is divided into four morpho-structural provinces (Figure 1a): (1) the Levantine province, a domain of salt-related folding; (2) the Eastern province, a domain of intense salt-related tectonics; (3) the Central province with pockmark fields and gas chimneys, distinguished by active sedimentary instability and fluid-related processes; and (4) the Western province with mud cones, characterized by active turbiditic processes, salt tectonics and fluid venting (Mascle et al. 2006; Huguen et al. 2009). The accumulation of organic-rich sediments, probably since the early

72 Cenozoic, led to the formation of hydrocarbons in deep reservoirs that were partially

73 sealed by the deposition of thick evaporites during the Messinian (Hsu et al. 1977). A

74 mixture of hydrocarbons, water and mud is expelled through faults that may extrude

75 salt deposits, which reach the seafloor (Loncke et al. 2004). Fluid seepage is

76 recorded in geological features such as mud cones, caldera-like depressions, gas

77 chimneys, brine pools and pockmarks (Gontharet et al. 2007; Bayon et al. 2009a).

78 Chemosynthesis-based communities have been observed in association with these

79 different features (Huguen et al. 2005; Zitter et al. 2005; Dupré et al. 2007).

80
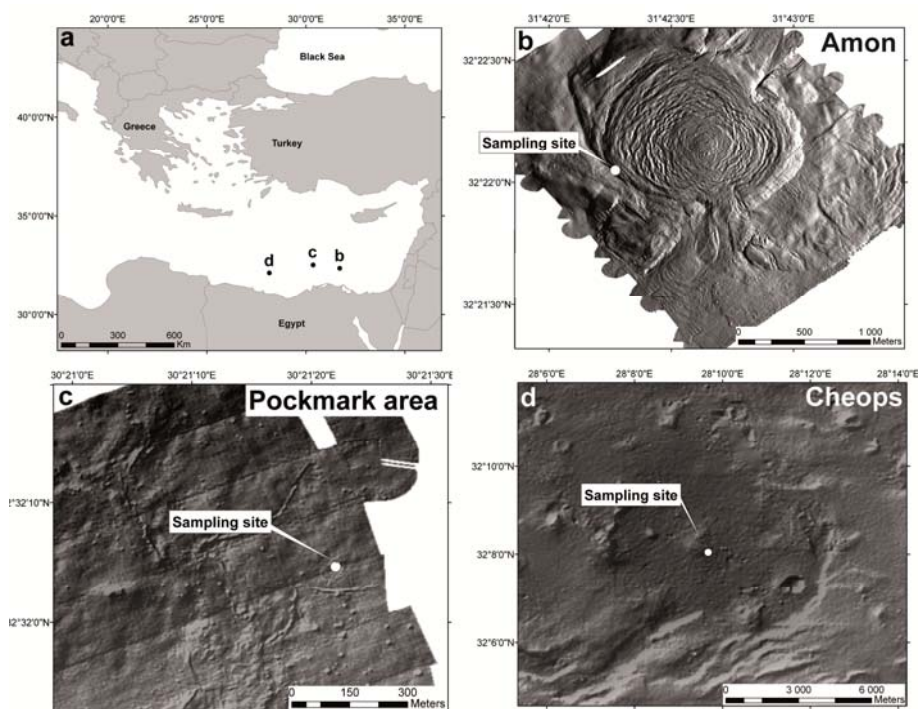


**Fig. 1** (a) General map of the Eastern Mediterranean Sea with the localisation of the sampling sites in the three morpho-structural provinces: (b) the Amon mud volcano (MV) located in the Eastern province; (c) the Pockmark area located in the Central province and, (d) the Cheops MV in the Western province. Sampling sites are indicated on each MVs

81

82 Faunal assemblages associated with Mediterranean cold seeps from the NDSF are

83 still relatively unknown. Only those from a few sites along the Mediterranean Ridge

84 have been described, and symbiont-bearing species such as the siboglinid

85 polychaete *Lamellibrachia anaximandri*, the lucinid *Lucinoma kazani* and the mytilid

86 *Idas modiolaefomis* were identified (Salas and Woodside 2002; Olu-Le Roy et al.

87 2004; Werne et al. 2004; Duperron et al. 2008; Southward et al. in press). The

88 distribution of fauna on the Amsterdam MV has been hypothesized to be linked to the

89  amount of methane escaping from the mud flows, which decreases from the summit

90  to the periphery (Olu-Le Roy et al. 2004). Likewise, biological zonation has also been

91  observed on the Barbados prism (Olu et al. 1997) and the Håkon Mosby MV

92  (Niemann et al. 2006; Jerosch et al. 2007). In both cases, the summit of the MV was

93  covered by fresh gassy mud flows and devoid of visible epifauna. Communities

94  dominated by sulphide oxidizing bacterial mats were observed close to the summit,

95  followed by symbiont-bearing fauna and heterotrophic fauna towards the periphery

96  (Olu et al. 1997; Zitter et al. 2003; Niemann et al. 2006; Jerosch et al. 2007). Fresh

97  mud flows are often characterized by very high rates of upward flux of reduced

98  sulphidic fluids, excluding animals (de Beer et al. 2006). Older mud flows, located at

99  the periphery, transport lower concentrations of methane and sustain sulphide

100 production, fueling chemosynthetic populations of siboglinid tubeworms or bivalves

101 like *Acharax*. The latter migrate to deeper sediment layers to reach for reduced

102 chemical compounds. This environment also constitutes a favorable habitat for

103 heterotrophic fauna, which develop in response to a local increase in microbial

104 production (Levin and Mendoza 2007).

105

106 The present study was the first opportunity to characterize the structure of the faunal

107 assemblages in the NDSF seeps on two types of geological features: MVs and

108 pockmarks. Prior to 2006, no ecological study had been performed on NDSF seep

109 sites, with the exception of a few observations and samples taken during the

110 NAUTINIL cruise in 2003 (Dupré et al. 2007; Bayon et al. 2009b; Huguen et al.

111 2009). The macro- and meiofaunal benthic communities associated with different

112 microhabitats found in three provinces of the NDSF were sampled by remotely

113 operated vehicles (ROVs) during two cruises: BIONIL in 2006 and MEDECO in 2007.

114 The microhabitats were characterized with regard to their environmental conditions

115 and faunal communities, mostly to family level. We then compared faunal

116 composition, density and diversity at local and regional scales to test the hypotheses

117 that 1) reduced habitats support higher biomasses but lower diversity of meio- and

118 macrofauna compared to surrounding oxygenated habitats, 2) carbonate crusts and

119 reduced sediments bear different faunal assemblages, 3) faunal composition is

120 related to microhabitat type rather than to the larger geological setting, 4) beta

121 diversity between the different microhabitats is related to differences in fluid flow and

122 substratum type.

123

## 2. Materials and methods

Faunal sampling and habitat characterizations were done during BIONIL M70/2b aboard the German R/V *Meteor* with the ROV *Quest4000* (MARUM, University Bremen) in November 2006 and during leg 2 of MEDECO aboard the French R/V *Pourquoi Pas?* with the ROV *Victor6000* (Ifremer) in November 2007.

129

### 2.1. Study sites

The cold seep sites from three of the four provinces of the NDSF were investigated: 1) the Amon MV in the Eastern province; 2) a carbonate cemented area close to a pockmark field associated with large debris-flows in the Central province; and 3) the Cheops MV in the Western province hosting large brine pools (Figure 1). A single reference sample located 15 km away from the centre of the Amon MV and outside the influence of fluid emissions, was sampled as a reference (hereafter marked "Ref") for oxygenated deep-sea sediments not associated with fluid flow.

138

### 2.1.1. The Western province – the Amon MV

The Amon MV (32°22'05"N – 31°42'27"E, Figure 1b) is circular, approximately 3 km in diameter, and 90 m high. It lies close to the limit of the Messinian platform, at 1150 m water depth. The summit is covered with mud blocks and clasts and shows a disturbed, chaotically structured surface suggesting recent impacts of mud extrusion and gas expansion. Temperatures at the centre reach 45°C at 10 m below the seafloor, confirming high upward fluid flow at this MV (Dupré et al. 2007; Dupré et al. 2008). The periphery of the Amon MV is characterized by highly bioturbated hemipelagic sediments. At its south-western rise, a lateral flow of reduced muds was identified ('sulphur-band') surrounded by carbonate crusts that were both sampled in 2006 during BIONIL. The carbonate crusts were rather thick, we could not observe blackish muds or siboglinid colonies associated with them.

151

### 2.1.2. The Central province – the Pockmark area

The Central province hosts large carbonate-cemented areas associated with reduced debris-flows, and numerous small pockmarks located between 1700 and 2100 m depth (Figure 1c). The pockmarks form circular depressions of a few meters in diameter and about 1 m deep, and are associated with the presence of authigenic

157 carbonate crusts and reduced sediments (Loncke et al. 2004). During BIONIL,
158 benthic communities were sampled from one reduced blackish sediments site at mid-
159 slope (site 2A, 32°32'00"N – 30°21'10"E, 1700 m) as well as from their surrounding
160 carbonate cements. These were directly associated with blackish muds, and living
161 siboglinid colonies were observed between the cracks of the flat, thin carbonates.
162
163 2.1.3. The Eastern province – the Cheops MV
164 The Cheops MV is located within the Menes caldera at 3000 m depth (32°08'05"N –
165 28°09'67"E, Figure 1d), above the Messinian platform. This caldera is a circular 50 m
166 deep depression 8 km in diameter. As previously observed in 2003 during the
167 NAUTINIL cruise, a mixture of brine and mud was flowing from Cheops during the
168 sampling operations in 2007 (MEDECO). The mud is expelled from deep layers as
169 indicated by high temperature anomalies (Huguen et al. 2009). This MV is also
170 characterized by numerous brine pools, covered by bright white matter, identified as
171 microbial sulphur deposits (Dupré et al. 2007; Omoregie et al. 2008). Brine pools
172 constitute direct evidence of fluid emissions, and the migration of fluids enriched in
173 salt induces high sediment instability that may influence faunal composition and
174 distribution on this MV. Faunal sampling and environmental characterizations were
175 carried out during MEDECO. Sparse carbonate crusts were observed but not
176 sampled.
177
178 2.2. Description of the microhabitats
179 At all cold seep sites visited, ROV surveys indicated a mosaic of visually
180 distinguishable microhabitats, characterized by the presence of visible fauna or
181 microbial mats. Two types of reduced habitats were sampled: 1) reduced blackish
182 sediments (Red) covered with whitish bacterial mats or small tubeworms at the
183 surface (Figures 2a, c, e) and 2) carbonate crusts (CC) that were dark-colored at
184 Amon, or "crumbly" and of whitish to light grey color at the Pockmark area Figures
185 2b, d).
186
187 Chemical characterization of the microhabitats was performed above the reduced
188 sediments of Cheops MV during MEDECO. Water samples were taken for chemical
189 analyses using the PEPITO water sampler above the organisms as close as possible
190 to the seafloor using the *Victor6000* manipulator arm. PEPITO collects water in 200

191    ml titanium bottles (Sarradin et al. 2009). Chemical measurements and sediment

192    samples were taken during BIONIL as close as possible above the seafloor or in soft

193    sediments with bottles (750 ml) and push cores (inner diameter 7.5 cm) at 2.5 to 50

194    m from the sampled microhabitats. Further sampling details are given in Table 1.

195
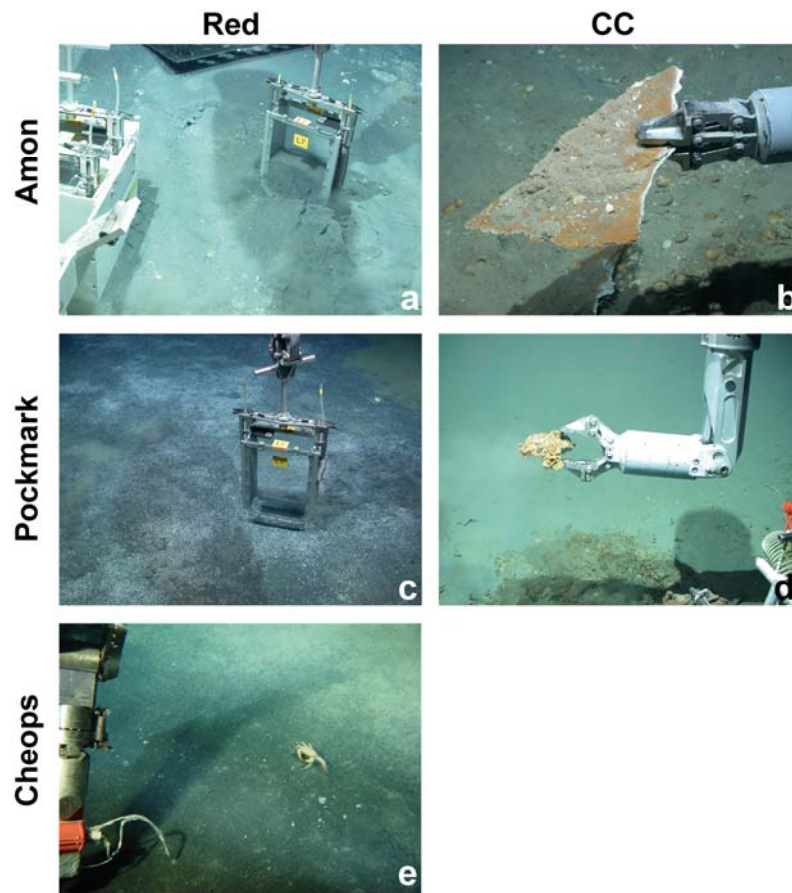


**Fig. 2** Representative photographs of the microhabitats sampled in the three study sites. On the Amon MV: (a) reduced sediments and (b) carbonate crusts; in the Pockmark area: (c) reduced sediments and (d) carbonate crusts; on the Cheops MV: (e) reduced sediments. Red: reduced sediments CC: carbonate crusts. All microhabitats were sampled during the BIONIL (2006) and MEDECO (2007) cruises. Photos a, b, c, d: MARUM, University Bremen, *QUEST4000* and photo e: Ifremer, *Victor6000*

196

197    Epi- and endofauna were sampled with blade corers on a surface of 200 cm² (Menot

198    et al. 2010) on all soft sediment sites (Figures 2a, c, d, g) and pieces of carbonate

199    crusts were sampled using the claw of the ROV *Victor6000* (Figures 2b, e). A

200    reference site 15 km away from the active centre of Amon has been sampled with a

201    single multicorer on which 3 tubes of a surface of 74 cm² were sampled (pseudo-

202    replicates). The number of samples for each microhabitat is reported in Table 1.

203 Quantitative sampling of the crusts was difficult because they had to be broken off in
204 pieces with the submersible manipulator. No crusts were obtained from Cheops.

205

206 2.3. Physico-chemical analyses

207 The 200 ml water samples were used to determine methane concentrations using the
208 technique of headspace sampling gas chromatography with a thermal-conductivity
209 detector (TCD) and a flame-ionisation detector (error of 4%; see method in Sarradin
210 and Caprais 1996).

211

212 Sediments from push corers were split horizontally at 1 cm intervals on board and
213 porewater was extracted by centrifugation of the different sediment layers. After
214 filtration and dilution, sulphate and chloride concentrations were measured by non-
215 suppressed anion exchange chromatography (Water IC-Pak anion exchange column,
216 waters 430 conductivity detector). Total dissolved sulphide concentrations were
217 determined with the diamine complexation method by colorimetric method (Cline
218 1969). Intact cores, along with supernatant water, were used for pH, oxygen and total
219 dissolved sulphide concentration measurements. Small-scale porewater
220 concentration profiles for $O_2$, $H_2S$, and pH were performed on push core samples
221 from soft sediments using microelectrodes as described in de Beer et al. (2006).
222 Microelectrodes with a tip diameter of ca. 20 μm were lowered into the sediment with
223 a step resolution of 200 μm to monitor the concentration profiles within the upper
224 sediment layer. Total oxygen consumption was measured *in situ* using a ROV-
225 operated benthic chamber module (Treude et al. 2009). The chamber encloses an
226 area of ca. 285 cm² together with approximately 10-15 cm of overlying bottom water.
227 The change in $O_2$ concentration over time in the enclosed water volume was
228 continuously monitored by two Clark-type mini-electrodes mounted in the chamber
229 lid. This measurement integrates all relevant transport and consumption processes
230 (diffusion, advection and fauna mediated transport as well as fauna respiration).

231

232 2.4. Faunal sorting and identification

233 The faunal samples were processed as described in Ritt et al. (2010). Sediments
234 from blade corers were photographed and split horizontally (0-1, 1-3, 3-5, 5-10, >10
235 cm) immediately after recovery. The range of the last slice depended on core lengths
236 that varied from 10 to 20 cm (Table1). Core slices were passed through a sieve

237  column (2 mm, 1 mm, 500 µm, 250 µm) and the retained sediment was preserved in
238  10% buffered formalin. In the laboratory, all sediments up to 10 cm below the
239  seafloor were rinsed and invertebrates were sorted under a dissecting microscope
240  and identified to the lowest taxonomic level possible (here mostly family level). In this
241  study, we considered macrofauna *sensu stricto* (>250 µm, Hessler and Jumars
242  1974), and any meiofaunal taxa such as Nematoda, Copepoda, Ostracoda and
243  Acarina were analysed separately. As a consequence, meiofaunal samples contain
244  only the largest fraction retained by a 250 µm mesh, and do not include the 32 µm or
245  62 µm size limit usual for meiofauna (Hessler and Jumars 1974; Thistle 2003; Van
246  Gaever et al. 2006).

247

248  The CC samples were preserved individually in 10% buffered formalin on board after
249  recovery. In the laboratory, the carbonates crusts were treated individually by
250  retrieving the organisms embedded or attached on them without breaking the
251  carbonate crusts. Then they were washed over a 250 µm mesh and the organisms
252  retained were processed as those on the soft sediments. The surface of the sampled
253  carbonate crusts were estimated using the IPLab Spectrum® image analysis
254  software. Quantitative 2-D surface analyses were performed on video images of the
255  upper face of the crusts, and we did it thrice to reduce error resulting from on-screen
256  tracing (Sarrazin and Juniper 1999). Total surface area was used to calculate area-
257  related indicators, such as density and biomass by counting organisms at both faces
258  and in the holes but divided the total of individuals only by the surface area.
259  However, because it does not take topography into account, this method may
260  underestimate total surface area and in turn overestimate density and biomass. The
261  crusts from the Pockmark area had a more complex topography with numerous holes
262  in comparison with the flat carbonates from Amon, hence, the two-side method may
263  have added to the uncertainty with areal estimates in this case.

264

265  2.5. Vertical distributions

266  Vertical distributions within each reduced sediment microhabitat and the reference
267  site were studied in the depth layers 0-1, 1-3, 3-5 and 5-10. Densities were calculated
268  by summing up the sediment layers up to 10 cm below the seafloor. This was
269  repeated for relative abundance and biomass.  Biomass was assessed by measuring
270  the mean preserved wet weight (pww) for each microhabitat. To do so, individuals of

271 all major macrofaunal taxa (bivalves, polychaetes, gastropods and crustaceans) were
272 pooled, pat-dried on absorbent paper and weighed on a microbalance with an error
273 of 0.1 mg.

274

275 2.6. Diversity measurements

276 Within-microhabitat ($\alpha$-diversity) and between-microhabitat ($\beta$-diversity) diversity
277 (Whittaker 1960; Gray 2000) were estimated for all microhabitats.

278

279 2.6.1. Alpha-diversity

280 The $\alpha$-diversity analyses were performed at the family level, which was reached for
281 most of the taxa except Zoantharia, Scyphozoa, Terebellida, Isopoda, Leptostraca,
282 Nematoda and Acarina. Undetermined families, individuals and larvae were removed
283 from the analysis because of the probability that they belong to a family already
284 listed. This may have resulted in an underestimation of the taxonomic richness.
285 Sample-based rarefaction curves (*sensu* Gotelli and Colwell 2001) were calculated
286 on macrofaunal datasets for each of the three study sites (Sanders 1968). Individual-
287 based rarefaction curves were also computed on macrofaunal datasets for each
288 microhabitat type, regardless of the province of origin. These curves plot expected
289 taxonomic richness against sampling effort and allow comparisons impossible with
290 observed richness (S). All rarefaction curves use the expected number of individuals
291 as the X-axis (Sanders 1968, corrected and modified by Hurlbert 1971; Gotelli and
292 Colwell 2001; Gauthier et al. 2010). Observed within-microhabitat taxonomic diversity
293 was evaluated using common diversity indices as well as more robust intrinsic-
294 diversity-based ordering methods (Liu et al. 2007; Gauthier et al. 2010). Commonly
295 used to define the $\alpha$ diversity, the taxonomic richness (*S*), the number of taxonomic
296 groups observed in each microhabitat, the Shannon's entropy ($H_e^{'}$; Shannon 1948)
297 and the Gini-Simpson diversity index ($D_{GS}$; Gini 1912; Simpson 1949) were
298 calculated. They are presented along with their *numbers equivalents*, allowing
299 straightforward comparisons between communities (Hill 1973; Patil and Taillie 1982;
300 Jost 2006; Jost 2007). Community evenness was also determined using Pielou's
301 index of evenness (*J'*; Pielou 1969).

302

303 The right tail-sum method (RTS) is a diversity ordering method, which is more robust
304 and stringent than other methods and allows graphical comparisons of communities
305 (Patil and Taillie 1982; Tothmérész 1998; Liu et al. 2007). Communities are ordered
306 in decreasing diversity from the top most curves to the lowest ones. No clear
307 conclusions can be drawn when curves intersect (Liu et al. 2007).

308

309 2.6.2. Beta-diversity

310 Despite the modest number of samples, multivariate analyses were conducted to
311 better illustrate the similarities and differences among faunal samples. The lowest
312 available taxonomic level was used. Principal component analysis (PCA) and Ward's
313 hierarchical clustering were used to indirectly evaluate the influence of habitat
314 conditions on community structure variation within and between the different
315 microhabitats and sites, but excluding the undetermined taxa as previously explained
316 for the alpha-diversity. A Procrustean randomization test (Jackson 1995) was
317 performed to compare the PCA results of the macrofaunal and meiofaunal datasets.
318 Abundance data were first Hellinger-transformed to conserve Hellinger, rather than
319 Euclidian, distances in PCA (Legendre and Gallagher 2001). Hellinger distances
320 were also used for Ward's hierarchical clustering. This distance gives low weight to
321 rare taxa in the analyses. In marine ecology in general, and even more so in the
322 deep-sea, rare species are not well sampled, and their sporadic appearance in
323 samples is mosly attributable to sampling error. In the PCA, the equilibrium
324 contribution circle was computed to identify the taxa having the most impact on the
325 position of the samples in the ordination (Legendre and Legendre 1998).

326 The Jaccard's similarity coefficient $\left(S_{jacc}\right)$ was used to quantify similarity in terms of
327 shared taxa among replicates within each microhabitat (Jaccard 1901); giving equal
328 weight to all taxa. Mean Jaccard similarity was computed to evaluate within-
329 microhabitat variation.

330

331 All analyses were performed in the R environment (R, Development Core Team,
332 2009). Rarefaction curves, diversity indices and diversity profiles were computed both
333 with the Biodiversity R package (Kindt and Coe 2005) and functions in Gauthier et al.
334 (2010). Multivariate analysis was carried out using the vegan package (Oksanen et
335 al. 2008).

336 3. Results

337 3.1. Physico-chemical characterization of microhabitats

338 The length of the cores varied from 10 to 20 cm depending on the nature of the
339 substratum (Table 1). All samples came from surface cold seep habitats at *in situ*
340 bottom water temperature of 13.5°C, as at the reference site. The Red cores from the
341 Pockmark area contained black sediments with a strong hydrogen sulphide odor. At
342 Amon, a horizon of 8-10 cm of black sediments overlaid grayish to beige hemipelagic
343 sediments. On Cheops, a black layer of only 1-2 cm was found on top of beige
344 hemipelagic sediments. The cores of the reference site contained only beige
345 sediments.

346

347 3.2. Chemical characterization at a larger scale around microhabitats

348 3.2.1. Bottom water measurements

349 Overall, the pH was slightly lower in reduced sediments than at the reference site
350 (Table 2). According to microprofiler measurements, pH value reached 7.9 at the
351 interface of reduced sediments on Amon while in the Pockmark area, it was around
352 8.1 (Table 2).

353

354 Oxygen bottom water concentrations were similar at all sites, including the reference
355 site (200-230 µmol $I^{-1}$) with the exception of the reduced sediments at Amon, where a
356 temporary depletion was observed, reaching values below 200 µmol $I^{-1}$. No free
357 sulphide was detected in the bottom waters at any of the sites, but sulphide was
358 found within the porewaters at two reduced sediment sites (Table 2). Low
359 concentrations of methane were measured in the bottom waters of Cheops and the
360 Pockmark area while they ranged between 3.6 and 9.3 µmol $I^{-1}$ in the overlying water
361 of Cheops samples (Table 2).

362

363 Sulphate values of 31 mmol $I^{-1}$ and chloride values of 529 mmol $I^{-1}$ were measured
364 above and throughout the core from the reference site. Sulphate and chloride
365 measurements above the reduced sediments on Amon showed values varying from
366 30 to 40 mmol $I^{-1}$ and 404 to 580 mmol $I^{-1}$ respectively (Table 2). Here, spatial
367 heterogeneity between samples was high, despite the proximity of the cores (few dm,
368 e.g. PC 46 and PC 47). In microbial mats from the Pockmark area, sulphate

369 concentrations varied from 29 to 30 mmol $l^{-1}$ while chloride values were high, ranging
370 from 606 to 630 mmol $l^{-1}$ (Table 2).

371

372 3.2.2. Porewaters, oxygen consumption and sulfate reduction rates in sediments
373 Oxygen penetration depth measured by microsensors was >4 cm at the reference
374 site (Table 2). The porewater samples from the reference site did not contain
375 sulphide or methane. Accordingly, sulphate reduction rate at the reference site was
376 not measurable, and oxygen consumption was <1 mmol $m^{-2}$ $d^{-1}$ (Table 2).

377

378 In contrast, oxygen microsensor profiles in reduced sediments of Amon, Cheops and
379 the Pockmark area showed complete oxygen consumption within the first 1-2
380 millimeters of seafloor (Figures 3a, b). Total dissolved sulphide profiles in reduced
381 sediments of Amon showed a maximum concentration of 2.5 mmol $l^{-1}$ at 12 cm depth
382 and were <0.8 mmol $l^{-1}$ in the top 5 cm (Table 2, Figure 3c). The profile suggested
383 that sulphide was oxidized completely within the first millimeters of sediment. In the
384 Pockmark area, sulphide concentrations at 12.5 cm depth reached 25 mmol $l^{-1}$
385 (Figure 3d), but sulphide was also completely consumed within the surface
386 sediments (Table 2). No porewater data were available for Cheops due to limitation in
387 dive time.

388

389 At the reference site off Amon, sulphate and chloride concentrations were
390 homogeneous along the whole length of the core with a mean of 32±2.4 mmol $l^{-1}$ for
391 sulphate and 530±49.5 mmol $l^{-1}$ for chloride (Figure 4a). On Amon reduced
392 sediments, sulphate and chloride profiles were homogeneous along the length of the
393 core reaching values similar to the reference sample with the exception of a high
394 sulphate concentration at the top of the core (Figure 4b). In the Pockmark area, the
395 consumption of sulphate was visible throughout the 16 cm of the core length,
396 whereas lower variation was observed in chloride (Figure 4c).
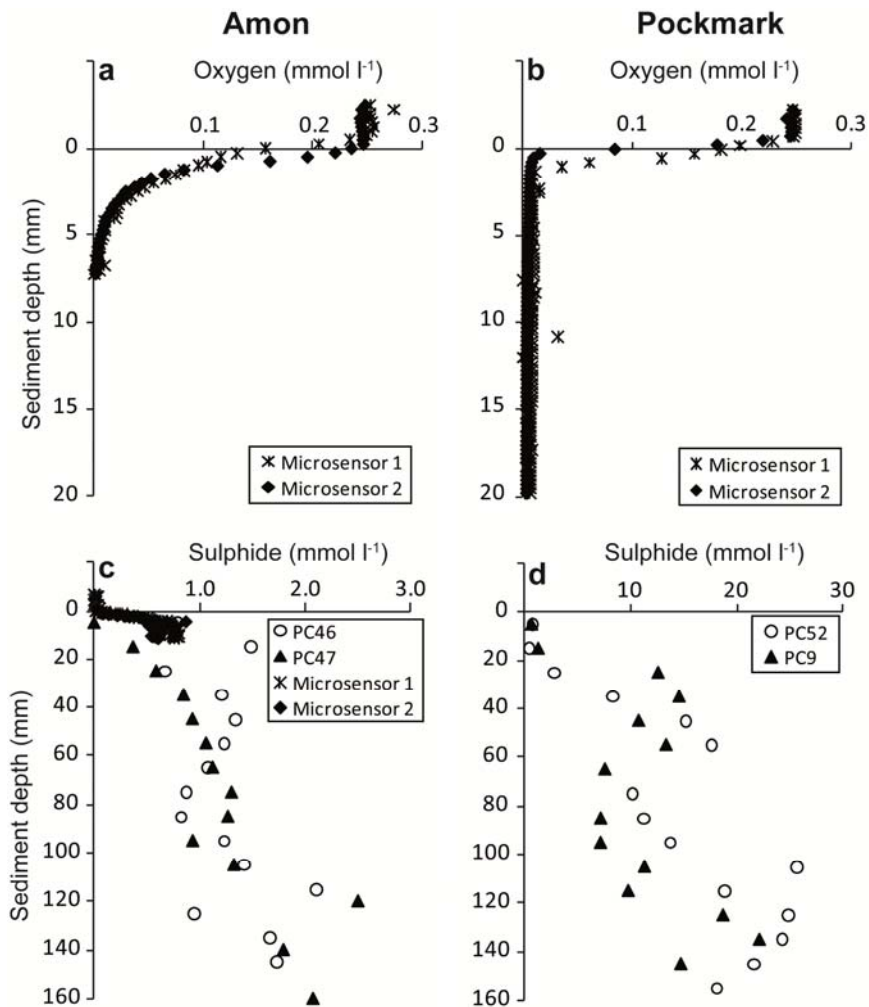
**Fig. 3** (a, b) Dissolved oxygen and (c, d) sulphide profiles measured by microsensors and in pore water extracted from push corers (PC) taken in reduced sediments on the (a, c) Amon MV and in (b, d) bacterial mats covering reduced sediments in the Pockmark area. The measurements were performed during the BIONIL cruise (2006)

Integrated sulphate reduction rates were negligible at the reference site, and low at the reduced sediment of Amon. Intermediate rates were measured for Cheops and high rates associated with the Pockmark area (Table 2). Likewise, total benthic oxygen fluxes were very low at the reference site, and 1-2 orders of magnitude higher at all reduced sediment sites, with the highest rates associated with the black sediments of the Pockmark area (Table 2).
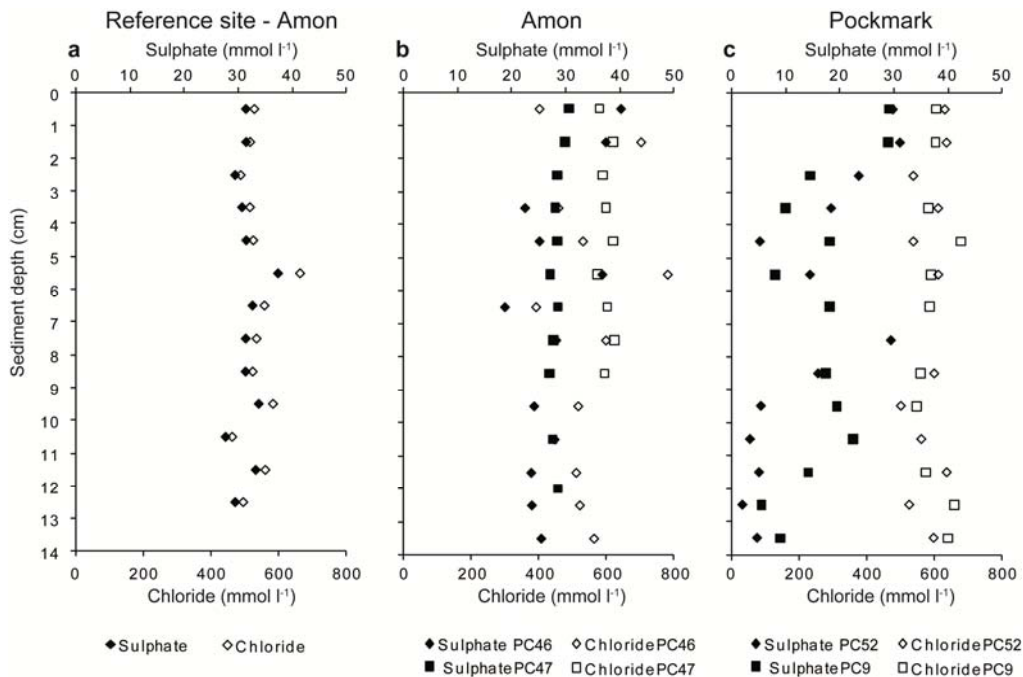
**Fig. 4** Sulphate and chloride profiles measured in porewater extracted from sediment cores sampled (a) at the reference site off Amon MV, (b) in reduced sediments on the Amon MV and, (c) in bacterial mats covering reduced sediments in the Pockmark area. The measurements were performed during the BIONIL cruise (2006)

404

405

406 3.3. Macro- and meiofaunal community description

407 3.3.1. Composition, abundance, density and $\alpha$-diversity patterns

408

409 Mean macrofaunal densities varied from 650 to 2,100 individuals m$^{-2}$ at Amon (Table

410 3), 1,950-3,500 individuals m$^{-2}$ in the Pockmark area (Table 43) and from 3,200 to

411 5,250 individuals m$^{-2}$ at Cheops (Table 4). This represents approximately 3.5%, 55%,

412 and 78% of the total fauna sampled at each site (Tables 5, 6). In comparison, the

413 fully oxic reference site had from 541 to 1,081 macrofaunal individuals m$^{-2}$ (Table 3),

414 which represented 67% of the total fauna. On the carbonate crust microhabitat (CC),

415 densities varied from 1,852 to 7,353 individuals m$^{-2}$ at Amon (Table 3) and from

416 1,852 to 7,353 individuals m$^{-2}$ in the Pockmark area (Table 4) representing

417 respectively 100% (except CC2 where it only represent 20%) and 63% of the fauna

418 sampled (Tables 3, 4).

419

420 Despite the large sieve mesh size used (250 μm), many specimens corresponding to

421 meiofaunal groups (copepods, ostracods, nematodes, mites) were found in our

422 samples (Tables 5, 6). Mean densities of meiofauna >250 μm varied from 31,800 to

75,550 individuals m$^{-2}$ at Amon (Table 5), 1,450 to 3,950 individuals m$^{-2}$ in the Pockmark area (Table 6) and reached 600 to 2,850 individuals m$^{-2}$ at Cheops (Table 6). At Amon, meiofaunal mean density was higher in reduced sediments compared to carbonate crusts (Table 5). Overall, nematodes dominated the meiofauna >250μm samples, varying from 95 to 100% of total abundances on the reduced sediments from the Amon and Cheops (Tables 5, 6). However, in the reduced sediments of the Pockmark area, nematodes represented only 36% of the meiofauna (Table 6). Here, harpacticoid copepods reached up to 37.5% of the meiofaunal abundance, followed by ostracods (~16%). Surprisingly, besides four nematodes, no meiofauna was sampled from the CC microhabitat of Amon, compared to a relatively high number of nematodes found at the CC of the Pockmark area (Tables 5, 6).

Relative faunal abundances varied between microhabitats and between replicate samples of the same microhabitat, especially on carbonate crusts. Overall, the steady increase of the individual-based rarefaction curves suggests that the sampling effort was not sufficient (Figure 5a). Only the curves of the reduced microhabitats of Cheops and the Pockmark area showed that we attained a relatively good estimation of their taxonomic richness. These curves also showed that the taxonomic richness between the different reduced sediment microhabitats was highest on Amon, followed by the Pockmark area and finally Cheops. The opposite trend was observed for the CC microhabitats, where the diversity was higher in the Pockmark area (Figure 5a). Since the ranking of the curves would probably remain the same with additional macrofaunal samples, we can conclude with confidence that the total family richness (S) on Amon was highest on reduced sediments, intermediate on the Reference site and lowest on CC, while the CC microhabitat in the Pockmark area was richer than the reduced sediments (Figure 5a; Tables 7, 8).

In terms of evenness (Pielou's index J', Table 8), the reference sample harbored the most even distribution followed by CC from the Pockmark area and reduced sediments from Amon (also shown in Figure 5b). Finally, Red from Cheops was the poorest microhabitat sampled in the NDSF. It was amongst the least even of all microhabitats along with CC from Amon and Red from Pockmark (Tables 7, 8). At Amon, polychaetes were the dominant taxa in the reduced habitats and reference samples, constituting respectively ~82% and 71% of total faunal abundance. A total

of 8 polychaete families or orders (since the Terebellida were not identified at the family level) were represented in the reduced sediments (Tables 3, 7). With ~11.5% of the total macrofaunal abundance, bivalves were the second dominant taxon in the reduced sediments of Amon, whereas cnidarians (~18%) ranked second in the reference sample. Gastropods and crustaceans were present in low abundance (<6%) in reduced sediments while on the reference samples, low abundances were for the crustaceans and sipunculians. On CC from Amon, cnidarians represented 72% of the total abundance, distantly followed by polychaetes (~17%; Table 8). Some gastropods and sipunculians were also present in low abundance (<6%; Table 3a). In the Pockmark area, reduced sediments were dominated by 8 polychaete taxa, reaching ~84% of the total macrofaunal abundance, followed by bivalves and gastropods (Tables 4, 7). Contrary to Amon, the fauna from CC in the Pockmark area was more evenly distributed with gastropods and polychaetes representing respectively ~51% and 40% of the total abundance (Table 4). Bivalves and crustaceans were also present, representing less than 8% of the total macrofaunal abundance (Table 4). The rarefaction curves and the Pielou's index confirm the higher evenness of the CC from the Pockmark area compared to CC from Amon (Figure 5a; Tables 7, 8), the highest evenness being observed on the reference site (Table 8). Finally, on Cheops, polychaetes largely dominated reduced sediments, with a mean of 96% of the faunal abundance, followed by low proportions of crustaceans and gastropods (Tables 4, 7).



**Fig. 5** (a) Rarefaction curves (b) and right tail-sum intrinsic diversity profiles for the pooled macrofaunal abundance data at the family level and at each microhabitat from the Amon MV (3 microhabitats including the reference sample), the Pockmark area (2 microhabitats) and the Cheops MV (1 microhabitat)

479    The RTS performed with the same dataset is difficult to interpret due to the crossing
480    of the curves (Figure 5b). Using this analysis, Amon reduced sediments were the
481    richest and most even microhabitat among the three reduced sediments. In contrast,
482    the CC from the Pockmark area was more diverse than that from Amon (Figure 5b).
483
484    Finally, we pooled the data obtained for the different microhabitats to determine the
485    diversity of each site, including the reference samples from Amon. For Amon and the
486    Pockmark area, the sample-based rarefaction curves did not level-off, suggesting
487    that sampling was insufficient to accurately estimate taxonomic richness (Figure 6a).
488    At Cheops, despite the low sample number (n=3), the curve leveled-off, suggesting
489    that its macrofaunal diversity was well described (Figure 6a). Our data indicate that
490    diversity was higher at microhabitats sampled on Amon, followed by the Pockmark
491    area, the reference samples from Amon and lastly, by Cheops (Figure 6a). Overall,
492    the distribution of macrofauna was relatively even on Amon, since the most abundant
493    taxon only reached ~30% for both active and reference sites, whereas the most
494    abundant taxon represented ~45% and ~55% on the Pockmark area and Cheops
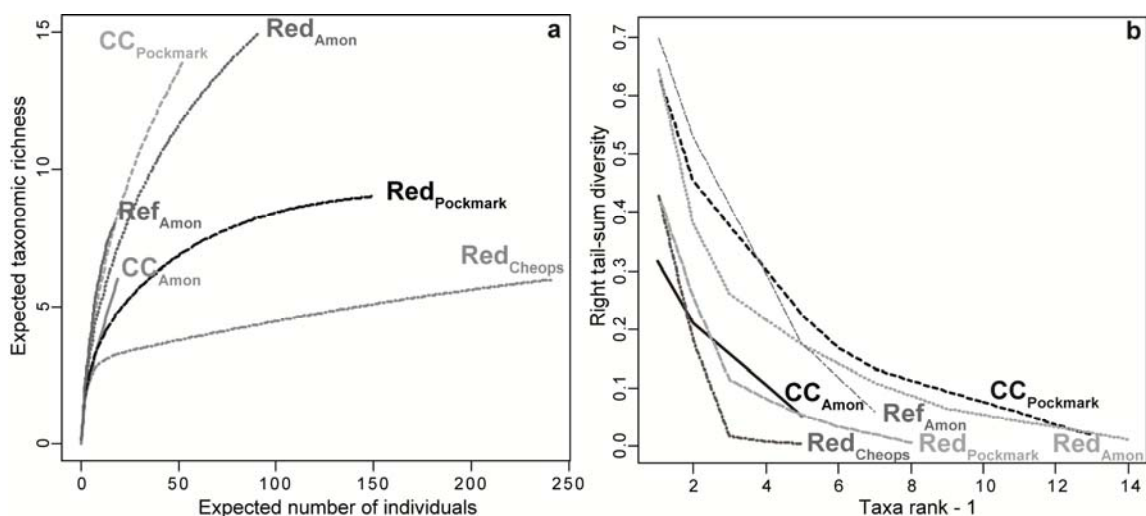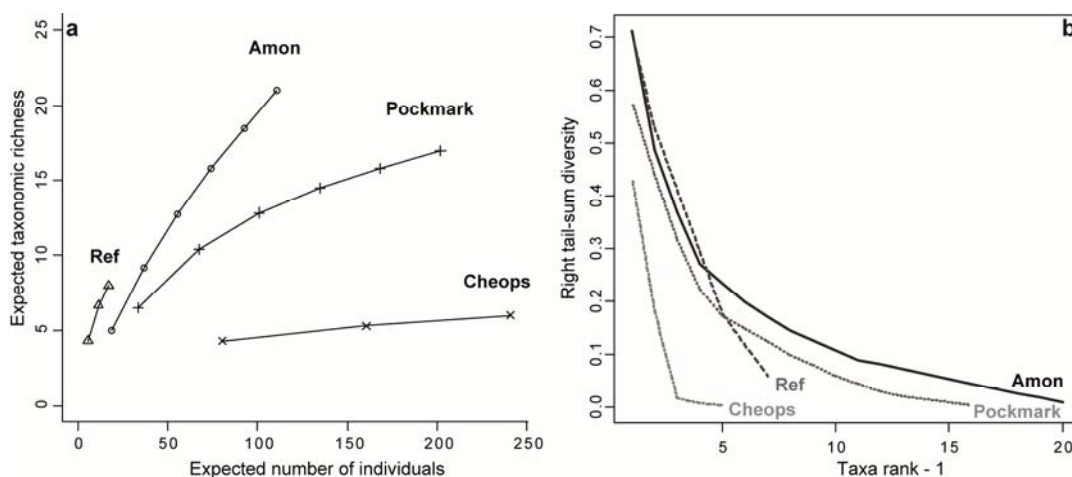495    respectively (Figure 6b).
496
497



**Fig. 6** (a) Rarefaction curves and (b) right tail-sum intrinsic diversity profiles for the pooled macrofaunal abundance data at the family level, according to the three study sites after pooling active microhabitats. Amon MV, n=6, Pockmark area n=3, and Cheops MV, n=3. The reference sample from Amon is reported separately, n=3 (Ref)

498
499
500
501

502 3.3.2. Symbiont-bearing fauna versus heterotrophic fauna

503 The symbiont-bearing fauna (for types of symbioses see Olu-Le Roy et al. 2004)
504 represented 17 to 36% of the total faunal abundance in the reduced sediments from
505 Amon, while the CC and the reference sample did not harbour any (Tables 7, 8). The
506 symbiont-bearing fauna was represented by Frenulata polychaetes as well as by four
507 bivalve species (*Lucinoma kazani*, *Idas modiolaeformis*, *Thyasira striata* and
508 *Isorropodon perplex*; Table 3). The Pockmark area had between 10 and 16% of
509 symbiont-bearing fauna both in the sediment and CC microhabitats, respectively
510 (Tables 5, 7, 8). This fauna was represented by two known bivalve species (*L. kazani*
511 and *I. perplexum*) and one unknown Lucinidae in the sediments. Only one bivalve
512 species was present in the CC microhabitat (*I. modiolaeformis*; Table 4). No
513 symbiont-bearing fauna was sampled at Cheops (Tables 7, 8) or at the reference
514 site.

515

516 3.3.3. Vertical distributions within the sediments

517 The distribution within the sediment layers down to 10 cm below the seafloor of the
518 macrofaunal relative abundances differed between the three reduced sediment
519 microhabitats (Figure 7a). At all reduced sediment sites, oxygen did not penetrate
520 deeper than a few mm, and sulfide concentration increased with sediment depth
521 below 2 cm to 1-2 mmol l$^{-1}$ at Amon and to 10-20 mmol l$^{-1}$ in sediments of the
522 Pockmark area. Hence, in the Pockmark area, the macrofauna was concentrated at
523 the uppermost layer [0-1 cm] with about 85% of the total abundance (Figure 7a).
524 However, some capitellid polychaetes and undetermined bivalves – that may be
525 vesicomyids and lucinids – were found in the [5-10 cm] layers. In the Cheops area,
526 the macrofauna was almost evenly distributed between the [0-1 cm] and [1-3 cm]
527 layers and only few spionid polychaetes were found in the [5-10 cm] layer. The profile
528 obtained for the reduced sediments of Amon was different, with a more
529 homogeneous distribution within the 10 cm layer and a relatively high abundance at
530 [5-10 cm] (Figure 7a) especially of frenulate, capitellid and dorvilleid polychaetes. At
531 the reference site, most macrofauna was concentrated in almost equal proportions in
532 the two first layers [0-1 cm] and [1-3 cm]. There, the distribution showed a clear
533 decrease with depth, as no organism was found at the [5-10 cm] layer (Figure 7a).
534 The meiofauna >250 μm also decreased with depth at the reference site, with up to
535 60% of the total meiofaunal abundance found in the two first layers (Figure 7b). The

536  same trend was observed in reduced sediments from Amon with this time almost
537  60% concentrated in the first layer. This pattern was different at the Pockmark area,
538  where the meiofaunal abundance was highest in the [3-5 cm] layer followed by the [1-
539  3 cm] and [5-10 cm] layers (Figure 7b). However, the few organisms found in the [5-
540  10 cm] layer consisted of nematodes at Amon, and of harpacticoid copepods at the
541  Pockmark area.
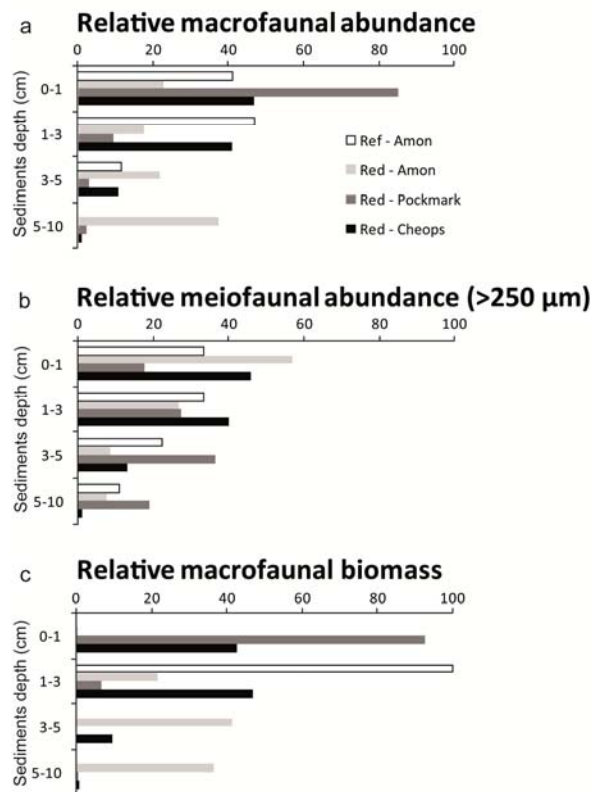


**Fig. 7** Vertical distribution of (a) macrofaunal and (b) meiofaunal (>250 μm) relative abundances and (c) macrofaunal relative biomass with depth after summing the three replicates (n=3) for each sediment layer of the reduced sediment microhabitats from Amon MV, Pockmark area and Cheops MV. The reference site from Amon is also included

542

543  In general, all soft sediments showed a low macrofaunal biomass, except the
544  reduced sediments of Amon where the mean biomass reached 0.12±0.1 kg pww m$^{-2}$
545  (Table 7). Here, the vertical distribution showed an increase with depth from 1 to 10
546  cm with about 40% of the total macrofaunal biomass remaining in the [5-10 cm] layer
547  (Figure 7c) due to the presence of few lucinid and thyasirid bivalves. In the reduced
548  sediments of the Pockmark area, most of the macrofaunal biomass (93%) was
549  observed within the top layer [0-1 cm] and mainly consisted of dorvilleid polychaetes.
550  Reduced sediments at Cheops hosted a similar biomass in the top two layers [0-1]

551  and [1-3 cm], with 43 and 47% of the total biomass respectively mainly represented
552  by hesionid, spionid, terebellid polychates and Leptostraca crustaceans. Next, a
553  sharp decrease was observed with depth (Figure 7c). At the reference site, mean
554  biomass was very low (Table 8), and integrally located within the [1-3 cm] layer
555  (Figure 7c) due to the presence of one sipunculian and few spionid polychaetes.

556

557  3.3.4. Beta diversity patterns
558  The first two components of the principal component analysis (PCA) on macrofaunal
559  data accounted for 41.7% of the variance in macrofaunal distribution (Figure 8a).
560  Three clusters appear in reduced space: the carbonate crust samples; the reduced
561  sediment samples except those from Cheops; and the Amon reference site and
562  Cheops reduced sediments samples. Thus the variability between microhabitats was
563  higher than that within the microhabitats, but lower than that among the geostructures
564  (Figure 8). Polychaete taxa (Spionidae, Terebellida, Dorvilleidae, Capitellidae) and
565  gastropods (Orbitestellidae) had the greatest impact on the variation in community
566  structure. Focusing on these taxa, they appeared to be indicative of different groups,
567  representing different types of microhabitats rather than different sampling locations.
568  In the first group, Spionidae and Terebellida highly contributed to the positioning of
569  the reduced sediments from Cheops and reference samples from Amon. In the
570  second group, Orbitestellidae highly contributed to the positioning of both carbonate
571  crust microhabitats (Pockmark and Amon). Finally Capitellidae and Dorvilleidae
572  presented high contributions in reduced sediments from Amon and Pockmark area
573  (Figure 8a). These three groups were also distinguished on the Ward's cluster
574  (Figure 8b). According to the datasets, the pooling of both carbonate crust
575  microhabitats seemed to be due to their low number of individuals (n=18 and 53)
576  rather than to the presence of shared taxa (Tables 3a, b). When regarding the
577  similarity level defined by the dotted line, the Ward's cluster also showed that the
578  reduced sediments from Cheops had higher similarities with the carbonate crust
579  microhabitats than with the other reduced sediment "soft" microhabitats (Figure 8b).

580

581  A PCA with Hellinger-transformed meiofaunal >250 µm data only (not shown)
582  exhibited the same general distance patterns as the one with macrofauna *sensu*
583  *stricto* (Procruste test stat=0.53, *p*=0.013, 1000 permutations). However, meiofaunal

584   sampling was very incomplete, especially on hard substratum, and these results
585   might reflect this paucity of observations.

586
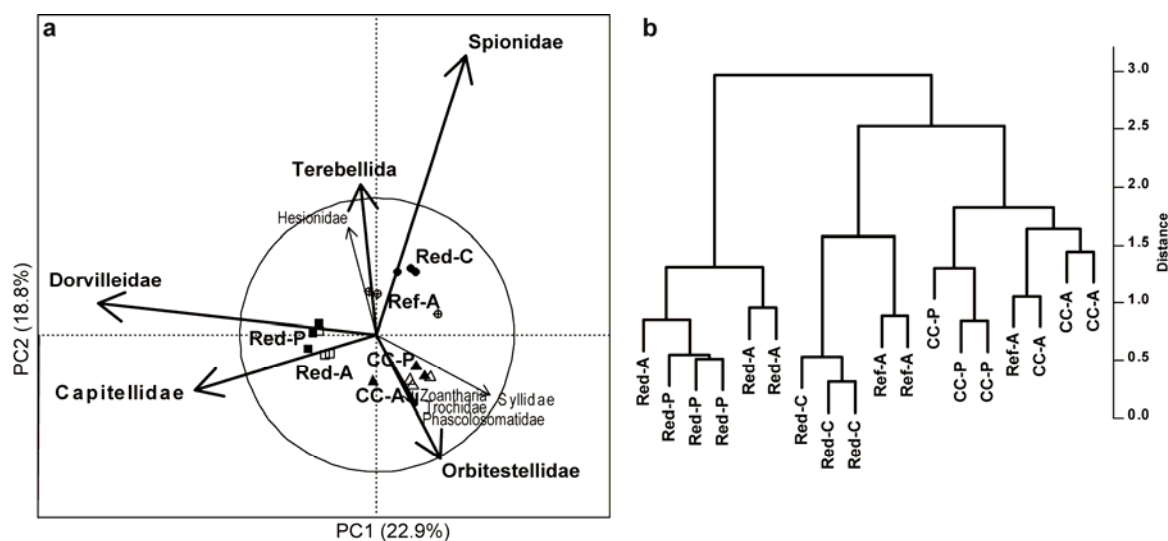


**Fig. 8** (a) Principal Component Analysis (PCA, scaling type 1) of Hellinger-transformed macrofaunal abundances on the Amon MV (A), Pockmark area (P) and the Cheops MV (C). The first two axes represent 41.7% of the total variance in macrofaunal abundance. The circle of equilibrium indicates the significant contribution of five taxa (radius=0.65). Vectors shorter than 0.34 were removed. (b) Ward's hierarchical clustering was performed with Hellinger-transformed macrofaunal abundances for each microhabitat types. Red: reduced sediments, CC: carbonate crusts, and Ref: reference sample

587

588

589   4. Discussion

590   This study investigated the differences in faunal diversity in relation to different

591   habitats and their biogeochemical conditions at three cold seep sites of the NDSF.

592   Due to inevitably limited submersible time, sampling effort was relatively low given

593   the high heterogeneity of cold seeps sites. Nevertheless, our results provide the first

594   insights on seep faunal composition and diversity and their relationships with

595   environmental conditions in the NDSF area.

596

597   4.1. Difference between the reference site and cold seep habitats at Amon MV

598

599   The reference site did not show any evidence of seepage whether direct (i.e. no

600   detection of methane and sulphide fluxes) or indirect (i.e. absence of symbiont-

601   bearing fauna). The fauna found at the reference site was different from that of the

602   reduced habitats and carbonate crusts from Amon. Densities of macro- and

603   meiofauna were two-fold lower than in reduced sediments, and total benthic oxygen

consumption was an order of magnitude lower. Accordingly, biomass was 1-4 orders of magnitude lower than at all other active sites from Amon. The reference site showed a relatively high evenness, but a lower diversity than the reduced sediment sites of Amon, therefore refuting our initial hypothesis. The reduced sediment microhabitats sampled within the present study support an overall higher faunal diversity compared to close-by oxygenated habitats. This pattern has already been observed on Eel River at about 500 m depth where diversity on clam beds was similar or higher than on non-seep sites (Levin et al. 2003; Levin et al. 2010). However, this is in contradiction with other studies from 770 to 3200 m depth were diversity appears to be lower at active seep sites (Sahling et al. 2002; Levin et al. 2010; Menot et al. 2010)

Comparing among sites, the relationship between seepage activity and diversity could best explained by a hump-shaped curve. We suggest that at the relatively low sulphide concentrations encountered at Amon the reduced sediments could be considered as an "ecotone" enhancing diversity by presenting a high variability of chemical environment and ecological niches, favoring the establishment of symbiont-bearing fauna but not limiting heterotrophic fauna by toxic concentrations of sulphide (Cordes et al. 2010). In contrast, the Pockmark area or similarily active seeps such as Hydrate ridge (Sahling et al. 2002) appear to show declined diversity, despite the high abundances/biomasses observed, potentially selecting for specialists able to withstand high sulfide concentrations and fluxes.


4.2. Reduced sediment microhabitats

The reduced sediment microhabitats were influenced by fluid emissions as attested by biogeochemical conditions. Sulphide concentrations at 12 cm below the seafloor in the Pockmark area were 10 times higher than what was observed on Amon for the same sediment depth. This flux was associated with a higher oxygen uptake and faster consumption at the water-sediment interface, suggesting higher microbial activity within reduced sediments of the Pockmark area compared to all other sites. According to a previous study (Girnth et al. 2010), some evidences of brine overflowing the sediments were recorded at Amon reduced sediments. However, the homogeneity of the chloride profiles at both sites does not support the presence of upward seepage of saline fluids as observed in some areas of Cheops.

637  Biogeochemical measurements indicate a ranking of activity with the Pockmark
638  reduced sediments as the most sulphidic habitat, followed by Amon and Cheops.

639

640  Accordingly, the reduced sediment microhabitats at Amon and the Pockmark area
641  were colonized by symbiont-bearing species, including sioglinid polychaetes and
642  bivalves (Vesicomyidae, Lucinidae, Mytilidae and Thyasiridae) as well as by dorvilleid
643  and capitellid polychaetes. The presence of these two families provides direct
644  evidence for fluid emissions as they are usually associated with areas rich in organic
645  matter and with sulphidic environments (Rouse and Fauchald 1997). Dorvilleid
646  polychaetes also dominate reduced sediment microhabitats from other seep sites at
647  1100 m depth in the Marmara Sea (Ritt et al. 2010), at 2020 m depth in the
648  Mediterranean Sea (Amsterdam MV, Ritt et al., in prep.) and at 500 m depth at the
649  Eel River off California (Levin et al. 2003). Large nematodes were abundant in the
650  reduced sediments of Amon, as previously observed on other mud volcanoes at 1220
651  (Van Gaever et al. 2006) and 5000 m depth (Olu et al. 1997).

652

653  The fauna in the reduced sediment microhabitat from Amon hosted the highest
654  abundance of symbiont-bearing species, and its macrofaunal taxonomic richness
655  was two times higher than in the Pockmark area. The bivalve species observed in the
656  Pockmark area either harbored sulphide-oxidizing endosymbionts such as *Lucinoma*
657  *kazani* and *Isorropodon perplexum* (Salas and Woodside 2002; Olu-Le Roy et al.
658  2004) or different types of symbionts as in the undetermined species *Idas sp.* Med,
659  (Duperron et al. 2008).

660

661  On Cheops, the reduced sediments sampled were located about 250 m away from a
662  brine lake which features extreme physico-chemical conditions. Methane
663  concentrations at the surface of the lake varied from 2.4 to 3.7 mmol $l^{-1}$ with
664  temperatures of 20-40°C and salinities 210 to 244 g $l^{-1}$ (Mastalerz, Harmegnies, pers.
665  com.). Sediment cores revealed a dark layer covering a layer of brown hemipelagic
666  sediments, suggesting the occurrence of a relatively recent sulphidic mud flow.
667  Sulfate reduction rates and oxygen consumption rates were considerably lower than
668  at the other sites, indicating a low sulphide flux, as confirmed by pore water
669  measurements. Accordingly, despite the detection of elevated methane
670  concentrations in the bottom waters of Cheops above the reduced sediments, no

671 symbiont-bearing fauna was observed. This microhabitat was dominated by spionid
672 (~2200 individuals m⁻²) or terebellid (~660 individuals m⁻²) polychaetes, commonly
673 found in sandy or muddy environments, from intertidal habitats to abyssal depths
674 (Rouse and Pleijel 2001). Dense Terebellida beds, especially the Ampharetidae
675 family have been observed at about 1100 m depth on the New Zealand margin
676 (Sommer et al. 2009) and in the Marmara Sea (Ritt et al. 2010), as well as at 770 m
677 at Hydrate Ridge off Oregon (Levin et al. 2010) where methane concentrations in the
678 bottom water reach up to 2 mmol l$^{-1}$ and 0.7 µmol l$^{-1}$, respectively for the first two first.
679 At Cheops, methane concentrations varied between 4 and 8 µmol l$^{-1}$. This suggests
680 that terebellids are able to inhabit a wide range of environmental conditions. Further
681 chemical measurements are needed to have a better understanding of the intriguing
682 processes occurring within reduced sediments on Cheops.
683
684 4.3. Carbonate crust microhabitats
685 As expected, the difference in substratum between the soft sediment and carbonate
686 crust microhabitats appears to influence the composition and distribution of the seep
687 fauna in the NDSF. Nevertheless, the clustering of the CC microhabitats from Amon
688 and the Pockmark area appears to be due to the low number of sampled individuals
689 rather than the presence of common taxa. Sampling efficiency on hard substrata
690 does not appear to be ideal as suggested by the high heterogeneity between
691 replicates and the low Jaccard's similarity coefficients obtained. However these
692 results may reflect the real heterogeneity of this habitat in terms of faunal
693 composition and spatial distribution. Visual observations showed that the carbonate
694 crusts sampled in the Pockmark area were associated with reduced sediments
695 whereas those from Amon did not appear to be located in the vicinity of an active
696 area. In addition, the crusts showed different facies and colour that may reflect
697 different fluid intensities and stages of evolution (Bayon et al. 2009a). For example,
698 the carbonates from the south-western part of Amon are thick, dark and cemented,
699 and can reach 1 m of thickness. They may have been formed in the distant past,
700 during a period of intense fluid emissions (Dupré et al. 2007). The absence of
701 symbiont-bearing fauna and the dark color of crusts — due to their exposure to
702 oxygen-rich bottom water and their iron and manganese oxide cover — corroborate
703 the hypothesis that these carbonates may be relatively old. Fluid emissions may be
704 very low on this part of Amon, explaining the absence of symbiont-bearing fauna. The

705   low faunal densities and biomass further support the fact that this environment is not

706   favorable, neither to symbiont-bearing fauna, nor to heterotrophic fauna.

707

708   The light-colored and crumbly carbonates from the Pockmark area differed

709   morphologically from the "inactive" crusts found on Amon as they seem to be

710   relatively young. The precipitation of authigenic carbonates is controlled by high

711   alkalinity of pore waters (Aloisi et al. 2002; Michaelis et al. 2002) due to the activity of

712   consortia of archaea and bacteria involved in the anaerobic oxidation of methane

713   (AOM) coupled to sulphate reduction (Boetius et al. 2000). Another by-product of

714   AOM is sulphide which may support sulphide-oxidizing symbionts of chemosynthetic

715   fauna such as the siboglinid polychaetes found beneath the crusts. In addition, the

716   methane concentrations were high, reaching >5 µmol $l^{-1}$. Siboglinids may contribute

717   to bio-irrigation and favor advection and diffusion processes that play a significant

718   role in carbonate precipitation (Bayon et al. 2009a).

719

720   4.4. Comparison between Amon, the Pockmark area and Cheops

721   The reduced sediment microhabitats appeared to be distributed along a gradient

722   related to seepage intensity and thus, to methane, oxygen and sulphide fluxes; with

723   the Pockmark area as the most intense seepage site. The fauna from the reduced

724   sediment microhabitats of the Pockmark area and Amon were rather similar and

725   highly influenced by the presence of symbiotic organisms as well as dorvilleid and

726   capitellid polychaetes, usually associated with organically enriched, reduced

727   environments (Rouse and Pleijel 2001). Both communities showed relatively similar

728   oxygen consumption rates. The taxonomic diversity was higher on Amon followed by

729   the Pockmark area and Cheops. However, the reduced sediments, associated with

730   the debris-flow of the Pockmark area, were more sulphidic and probably also more

731   stable than the fresh Amon mud flow. The lower diversity and biomass observed in

732   the reduced sediments of the Pockmark could be due to the high level of sulphide

733   flux limiting the survival of most benthic species.

734

735   At the time of sampling, the mud flow at Cheops was probably recent as only a very

736   thin sulphidic horizon was observed on top of hemipelagic sediments. These

737   conditions may explain the lower diversity and the lack of symbiont-bearing fauna on

738   the sampling site located 250 m away from the central brine lake. According to video

739  observations, instability seems to decrease from the summit toward the periphery as
740  suggested by the presence of carbonate crusts with symbiont-bearing mytilids at
741  about 700 m away from the lake.

742

743  4.5. Comparison at a larger scale

744  In terms of seepage activity, Amon is comparable to the Håkon Mosby MV (1200 m
745  depth) from the Norwegian margin and the Amsterdam MV (2020 m depth) located
746  on the Mediterranean Ridge. These MVs discharge mud, fluids and gases from their
747  summits, which undergo episodic mud eruptions (Zitter et al. 2005; Dupré et al. 2007;
748  Feseker et al. 2008). This activity induces instability and chemical gradients that
749  influence the distribution of fauna, which is concentrically distributed around a chaotic
750  summit (Zitter et al. 2005; Jerosch et al. 2007). The reduced site sampled at Amon
751  was located on the base of the mud volcano, and influenced by lateral brine and mud
752  flows (Girnth et al. 2011). Interestingly, the dimensions of the reduced sediment site
753  was rather small (ca. 250 m) and the next larger reduced sediment patches were >2
754  km away.

755

756  The carbonate crusts and reduced sediments of the Pockmark area from the NDSF
757  showed similarities with a more recently discovered site, the giant REGAB pockmark
758  in the Gulf of Guinea at 3160 m depth. There, carbonate crusts are colonized by
759  dense mussel beds and siboglinid assemblages (Olu-Le Roy et al. 2007). Pockmark
760  and carbonate crust areas have also been observed at 740 m depth on the Storegga
761  slide and the Nyegga area located on the north-west of the Norway margin which
762  have undergone slide events. There, benthic fauna is represented by Siboglinidae,
763  Crinoidae, Pycnogonidae and microbial mats (Hovland et al. 2005; Hovland and
764  Svensen 2006; Paull et al. 2008). However, these features are taller than those
765  observed in the central province of the NDSF as they reach 190 m long and 40 m
766  wide, while pockmarks do not exceed a few meters in diameter at the NDSF study
767  site.

768

769  The Cheops MV share similarities with the Napoli MV located on the Mediterranean
770  Ridge at 1900 m depth, as they both harbor brine seepages (Charlou et al. 2003).
771  However, faunal density and taxonomic richness on Cheops are lower than those
772  observed on Napoli (Ritt et al., in prep). Faunal composition and distribution may be

773  strongly linked to the activity of the MV. Mud flows may initiate higher sedimentary
774  and chemical instabilities on Cheops, limiting the colonization of benthic species.
775  Although considered as an extreme habitat, the vicinity of brine lakes can be
776  colonized by dense colonies of Porifera as observed on Napoli (Ritt, pers obs) or by
777  dense mussel communities, such as those found on the shoreline of brine pools in
778  the Gulf of Mexico at 650 m depth (Macdonald et al. 1990; Smith et al. 2000). The
779  absence of dense assemblages of symbiont-bearing fauna close to the brines on
780  Cheops was thus unexpected and may be explained by the effect of recent
781  disturbances.

782

783  In conclusion, our comparative investigation of active cold seeps on the NDSF
784  suggested that seepage activity substantially enhanced benthic activity, biomass and
785  diversity compared to the surrounding oxygenated and oligotrophic deep-sea
786  environments. The biomass and biogeochemical activity of seep associated
787  communities is 1-2 orders of magnitude higher than the surrounding and diversity
788  was increased by a factor of 1.5. Reduced sediment microhabitats exhibited highest
789  biomasses and diversity in comparison with surrounding oxygenated areas
790  (reference site). As expected, reduced sediments and carbonate crusts were
791  characterized by distinct faunal composition and faunal similarities were observed
792  within each microhabitat type regardless of the site and geological structure (i.e. mud
793  volcano, pockmark). However, our heterogeneous results on carbonate crusts require
794  more investigation and emphasize the importance of developing a specific sampling
795  tool dedicated to hard substratum in the deep sea. No simple relationship was
796  detected between chemical conditions, sediment instability, fluid intensity and
797  community structure although there seems to be a gradient related to seepage
798  intensity between the different sites (Pockmark>Amon>Cheops). Further
799  investigations with an appropriate sampling strategy, especially regarding the
800  meiofauna, may help in highlighting the links between faunal distribution and
801  environmental conditions in the NDSF. Most likely, temporal dynamics in such active
802  geological systems may be very important in structuring community diversity. It could
803  be studied in the future by deploying autonomous video cameras and sensors as well
804  as by regularly monitoring a same site. Time-series data would help determine the
805  response of the fauna to instabilities and disturbances induced by the occurrence of

mud flows or brine seepage, and in which ways local diversity is related to temporal fluctuations and stability of habitats.

**References**

Aloisi G, Bouloubassi I, Heijs SK, Pancost RD, Pierre C, Sinninghe Damste JS, Gottschal JC, Forney LJ, Rouchy JM (2002) $CH_4$-consuming microorganisms and the formation of carbonate crusts at cold seeps. Earth and Planetary Science Letters 203: 195-203

Baker MC, Ramirez-Llodra EZ, Tyler P, German CR, Boetius A, Cordes EE, Dubilier N, Fisher CR, Levin LA, Metaxas A, Rowden AA, Santos RS, Shank TM, Van Dover CL, Young CM, Warén A (2010) Biogeography, Ecology, and Vulnerability of Chemosynthetic Ecosystems in the Deep Sea. In: McIntyre A (ed) Life in the World's Oceans: Diversity, Distribution, and Abundance. Wiley-Blackwell, pp 384

Bayon G, Henderson GM, Bohn M (2009a) U-Th stratigraphy of a cold seep carbonate crust. Chemical Geology 260: 47-56

Bayon G, Loncke L, dupre S, ducassou E, Duperron S, Etoubleau J, Foucher JP, Fouquet Y, Gontharet S, Huguen C, Klaucke I, Mascle J, Olu-Le Roy K, Ondreas H, Pierre C, Sibuet M, Stadnitskaia A, Woodside J (2009b) Multi-discinplinary investigations of fluid seepage on an unstable margin: The case of the Central Nile deep sea fan. Marine Geology 261: 92.104

Bellaiche G, Loncke L, Gaullier V, Mascle J, Courp T, Moreau A, Radan S, Sardou O (2001) The Nile Cone and its channel system: new results after the Fanil cruise. Comptes Rendus De L'Academie Des Sciences Série II Fascicule a-Sciences De La Terre Et Des Planètes 333: 399-404

Boetius A, Ravenschlag K, Schubert CJ, Rickert D, Widdel F, Gieseke A, Amann R, Jorgensen BB, Witte U, Pfannkuche O (2000) A marine microbial consortium apparently mediating anaerobic oxidation of methane. Nature 407: 623-626

Campbell KA (2006) Hydrocarbon seep and hydrothermal vent paleoenvironments and paleontology: Past developments and future research directions. Palaeogeography Palaeoclimatology Palaeoecology 232: 362-407

Charlou JL, Donval JP, Zitter T, Roy N, Jean-Baptiste P, Foucher JP, Woodside J (2003) Evidence of methane venting and geochemistry of brines on mud volcanoes of the eastern Mediterranean Sea. Deep Sea Research Part I: Oceanographic Research Papers 50: 941-958

Cita MB, Ryan WBF, Paggi L (1981) Prometheus mud breccia. An example of shale diapirism in the western Mediterranean Ridge. Ann. geol. Des Pays Hell. 13: 37-49

Cline JD, (1969) Spectrophotometric Determination of Hydrogen Sulfide in Natural Waters. Limnology and Oceanography 14: 454-458

Cordes EE, Becker EL, Hourdez S, Fisher CR (2010) Influence of foundation species, depth, and location on diversity and community composition at Gulf of Mexico lower-slope cold seeps. Deep Sea Research Part II: Topical Studies in Oceanography 57: 1870-1881

Dando PR, Austen MC, Burke RA, Kendall MA, Kennicutt MC, Judd AG, Moore DC, Ohara SCM, Schmaljohann R, Southward AJ (1991) Ecology of a North-Sea Pockmark with an active methane seep. Marine Ecology-Progress Series 70: 49-63

de Beer D, Sauter E, Niemann H, Kaul N, Foucher JP, Witte U, Schlüter M, Boetius A (2006) In situ fluxes and zonation of microbial activity in surface sediments of the Hâkon Mosby mud volcano. Limnology and Oceanography 51: 1315-1331

Dimitrov LI (2002) Mud volcanoes - the most important pathway for degassing deeply buried sediments. Earth-Science Reviews 59: 49-76

Duperron S, Halary S, Lorion J, Sibuet M, Gaill F (2008) Unexpected co-occurrence of six bacterial symbionts in the gills of the cold seep mussel Idas sp (Bivalvia : Mytilidae). Environmental Microbiology 10: 433-445

Dupré S, Buffet G, Mascle J, Foucher JP, Gauger S, Boetius A, Marfia C (2008) High-resolution mapping of large gas emitting mud volcanoes on the Egyptian continental margin (Nile Deep Sea Fan) by AUV surveys. Marine Geophysical Researches 29: 275-290

Dupré S, Woodside J, Foucher JP, de Lange G, Mascle J, Boetius A, Mastalerz V, Stadnitskaia A, Ondreas H, Huguen C, Harmegnies FO, Gontharet S, Loncke L, Deville E, Niemann H, Omoregie E, Roy KOL, Fiala-Medioni A, Dahlmann A, Caprais JC, Prinzhofer A, Sibuet M, Pierre C, Sinninghe Damste JS (2007)

Seafloor geological studies above active gas chimneys off Egypt (Central nile deep sea fan). Deep-Sea Research Part I-Oceanographic Research Papers 54: 1146-1172

Feseker T, Foucher JP, Harmegnies F (2008) Fluid flow or mud eruptions? Sediment temperature distributions on Håkon Mosby mud volcano, SW Barents Sea slope. Marine Geology 247: 194-207

Foucher JP, Westbrook GK, Boetius A, Ceramicola S, Dupre S, Mascle J, Mienert J, Pfannkuche O, Pierre C, Praeg D (2009) Structure and Drivers of Cold Seep Ecosystems. Oceanography 22: 92-109

Gauthier O, Sarrazin J, Desbruyères D (2010) Measure and mis-measure of species diversity in deep-sea chemosynthetic communities. Marine Ecology Progress Series 402: 285-302

Gini C (1912) Variabilità e Mutabilità. Tipographia di Paolo Cuppini, Bologna

Gontharet S, Pierre C, Blanc-Valleron MM, Rouchy JM, Fouquet Y, Bayon G, Foucher JP, Woodside J, Mascle J (2007) Nature and origin of diagenetic carbonate crusts and concretions from mud volcanoes and pockmarks of the Nile deep-sea fan (eastern Mediterranean Sea). Deep-Sea Research Part II-Topical Studies In Oceanography 54: 1292-1311

Gotelli NJ, Colwell RK (2001) Quantifying biodiversity: procedures and pitfalls in the measurement and comparison of species richness. Ecology Letters 4: 379-391

Gray JS (2000) The measurement of marine species diversity, with an application to the benthic fauna of the Norwegian continental shelf. Journal Of Experimental Marine Biology And Ecology 250: 23-49

Girnth A-C, Grünke S, Lichtschlag A, Felden J, Knittel K, Wenzhöfer F, de Beer D, Boetius A (2011) A novel, mat-forming Thiomargarita population associated with a sulfidic fluid flow from a deep-sea mud volcano. Environmental Microbiology 13: 495-505

Grünke S, Felden J, Lichtschlag A, Girnth A-C, Wenzhöfer F, de Beer D, Boetius A (in press) Niche differentiation among mat-forming, sulfide-oxidizing bacteria at cold-seeps of the Nile Deep Sea Fan (Eastern Mediterranean Sea). Geobiology 9

Hessler RR, Jumars PA (1974) Abyssal community analysis from replicate box cores in the central North Pacific. Deep Sea Research 21: 185-209

Hill MO (1973) Diversity and Evenness: A unifying notation and its consequences. Ecology 54: 427-432

Hovland M, Gardner JV, Judd AG (2002) The significance of pockmarks to understanding fluid flow processes and geohazards. Geofluids 2: 127-136

Hovland M, Svensen H (2006) Submarine pingoes: Indicators of shallow gas hydrates in a pockmark at Nyegga, Norwegian Sea. Marine Geology 228: 15-23

Hovland M, Svensen H, Forsberg CF, Johansen H, Fichler C, Fossa JH, Jonsson R, Rueslatten H (2005) Complex pockmarks with carbonate-ridges off mid-Norway: Products of sediment degassing. Marine Geology 218: 191-206

Hsu KJ, Montadert L, Bernoulli D, Cita MB, Erickson A, Garrison RE, Kidd RB, Melieres F, Muller C, Wright R (1977) History Of Mediterranean Salinity Crisis. Nature 267: 399-403

Huguen C, Foucher JP, Mascle J, Ondreas H, Thouement M, Stadnitskaia A, Pierre C, Bayon G, Loncke L, Boetius A, Bouloubassi I, De Lange G, Caprais JC, Fouquet Y, Woodside J, Dupre S, and the NAUTINIL Scientific Party (2009) Menes Caldera, a highly active site of brine seepage in the Eastern

Mediterranean Sea: "In situ" observations from the NAUTINIL expedition (2003) Marine Geology 261: 138-152

Huguen C, Mascle J, Woodside J, Zitter T, Foucher JP (2005) Mud volcanoes and mud domes of the Central Mediterranean Ridge: Near-bottom and in situ observations. Deep Sea Research Part I: Oceanographic Research Papers 52: 1911

Hurlbert SH (1971) The nonconcept of species diversity: A Critique and Alternative Parameters. Ecology 52: 577-586

Jaccard P (1901) Distribution de la flore alpine dans le Bassin des Dranses et dans quelques régions voisines. Bulletin de la société vaudoise des sciences naturelles

Jackson DA (1995) PORTEST: a PROcustean randomization TEST of community environment concordance. Ecosciences 2: 297-303

Jerosch K, Schluter M, Foucher JP, Allais AG, Klages M, Edy C (2007) Spatial distribution of mud flows, chemoautotrophic communities, and biogeochemical habitats at Hakon Mosby Mud Volcano. Marine Geology 243: 1-17

Jost G (2007) Partitioning diversity into independant alpha and beta components. Ecology 88: 2427-2439

Jost L (2006) Entropy and diversity. Oikos 113: 363-375

Judd AG, Hovland M (2007) Seabed fuid flow - The impact on geology, biology and the marine environment

Kindt R, Coe R (2005) Tree diversity analysis. A manual and software for common statistical methods for ecological and biodiversity studies. World Agroforestry Centre (ICRAF), Nairobi

Kopf AJ (2002) Significance of mud volcanism. Reviews of Geophysics 40: 52

Legendre P, Gallagher ED (2001) Ecologically meaningful transformations for ordination of species data. Oecologia 129: 271-280

Legendre P, Legendre L (1998) Numerical ecology, 2nd English ed.

Levin LA, Mendoza GF, Gonzalez JP, Thurber AR, Cordes EE (2010) Diversity of bathyal macrofauna on the northeastern Pacific margin: the influence of methane seeps and oxygen minimum zones. Marine Ecology 31: 94-110

Levin LA (2005) Ecology of cold seep sediments: Interactions of fauna with flow, chemistry and microbes Oceanography And Marine Biology - An Annual Review, Vol. 43. Crc Press-Taylor & Francis Group, Boca Raton, pp 1-46

Levin LA, Mendoza GF (2007) Community structure and nutrition of deep methane-seep macrobenthos from the North Pacific (Aleutian) Margin and the Gulf of Mexico (Florida Escarpment). Marine Ecology-An Evolutionary Perspective 28: 131-151

Levin LA, Ziebis W, Mendoza GF, Growney VA, Tryon MD, Mahn C, Gieskes JM, Rathburn AE (2003) Spatial heterogeneity of macrofauna at northern California methane seeps: influence of sulfide concentration and fluid flow. MEPS 265: 123-139

Liu C, Whittaker RJ, Ma K, Malcolm JR (2007) Unifying and distinguishing diversity ordering methods for comparing communities. Population Ecology 49: 89-100

Loncke L, Mascle J, and the Fanil Scientific Party (2004) Mud volcanoes, gas chimneys, pockmarks and mounds in the Nile deep-sea fan (Eastern Mediterranean): geophysical evidences. Marine and Petroleum Geology 21: 669

Macdonald IR, Reilly JF, Guinasso NL, Brooks JM, Carney RS, Bryant WA, Bright TJ (1990) Chemosynthetic mussels at a brine-filled pockmark in the Northern Gulf of Mexico. Science 248: 1096-1099

Mascle J, Sardou O, Loncke L, Migeon S, Camera L, Gaullier V (2006) Morphostructure of the Egyptian continental margin: Insights from swath bathymetry surveys. Marine Geophysical Researches 27: 49-59

Mascle J, Zitter T, Bellaiche G, Droz L, Gaullier V, Loncke L (2001) The Nile deep sea fan: preliminary results from a swath bathymetry survey. Marine and Petroleum Geology 18: 471-477

Menot L, Galéron J, Olu K, Caprais JC, Crassous P, Khripounoff A, Sibuet M (2010) Spatial heterogeneity of macrofaunal communities in and near a giant pockmark area in the deep Gulf of Guinea. Marine Ecology 31:78-93

Michaelis W, Seifert R, Nauhaus K, Treude T, Thiel V, Blumenberg M, Knittel K, Gieseke A, Peterknecht K, Pape T, Boetius A, Amann R, Jorgensen BB, Widdel F, Peckmann JR, Pimenov NV, Gulin MB (2002) Microbial reefs in the Black Sea fueled by anaerobic oxidation of methane. Science 297: 1013-1015

Milkov AV (2000) Worldwide distribution of submarine mud volcanoes and associated gas hydrates. Marine Geology 167: 29-42

Niemann H, Losekann T, de Beer D, Elvert M, Nadalig T, Knittel K, Amann R, Sauter EJ, Schluter M, Klages M, Foucher JP, Boetius A (2006) Novel microbial communities of the Haakon Mosby mud volcano and their role as a methane sink. Nature 443: 854-858

Oksanen J, Kindt R, Legendre P, O'Hara B, Simpson GL, Solymos P, Henry M, Stevens H, Wagner H (2008) Vegan: Community Ecology Package. R package version 1.15-1., pp http://cran.r-project.org/, http://vegan.r-forge.r-project.org/

Olu-Le Roy K, Caprais JC, Fifis A, Fabri MC, Galeron J, Budzinsky H, Le Menach K, Khripounoff A, Ondreas H, Sibuet M (2007) Cold-seep assemblages on a giant pockmark off West Africa: spatial patterns and environmental control. Marine Ecology-an Evolutionary Perspective 28: 115-130

Olu-Le Roy K, Sibuet M, Fiala-Medioni A, Gofas S, Salas C, Mariotti A, Foucher J-P, Woodside J (2004) Cold seep communities in the deep eastern Mediterranean Sea: composition, symbiosis and spatial distribution on mud volcanoes. Deep Sea Research Part I: Oceanographic Research Papers 51: 1915

Olu K, Lance S, Sibuet M, Henry P, Fiala-Medioni A, Dinet A (1997) Cold seep communities as indicators of fluid expulsion patterns through mud volcanoes seaward of the Barbados accretionary prism. Deep Sea Research Part I: Oceanographic Research Papers 44: 811

Omoregie EO, Mastalerz V, de Lange G, Straub KL, Kappler A, Roy H, Stadnitskaia A, Foucher JP, Boetius A (2008) Biogeochemistry and community composition of iron- and sulfur-precipitating microbial mats at the Chefren mud volcano (Nile Deep Sea fan, Eastern Mediterranean). Applied And Environmental Microbiology 74: 3198-3215

Patil GP, Taillie C (1982) Diversity as a Concept and its Measurement. Journal of the American Statistical Association 77: 548-561

Paull CK, Hecker B, Commeau R, Freeman-Lynde RP, Neumann C, Corso WP, Golubic S, Hook JE, Sikes E, Curray J (1984) Biological communities at the Florida Escarpment resemble hydrothermal vent taxa. Science 226: 965-967

Paull CK, Ussler W, Holbrook WS, Hill TM, Keaten R, Mienert J, Haflidason H, Johnson JE, Winters WJ, Lorenson TD (2008) Origin of pockmarks and

chimney structures on the flanks of the Storegga Slide, offshore Norway. Geo-Marine Letters 28: 43-51

Pielou EC (1969) An introduction to mathematical ecology, New York

R Development Core Team (2009). R: A language and environment for statistical computing. R Foundation for Statistical Computing, Vienna, Austria

Ritt B, Desbruyeres D, Caprais JC, Khripounoff A, Le Gall C, Gauthier O, Buscail R, Olu K, Sarrazin J (in prep.) Cold seep communities in the deep eastern Mediterranean Sea: Composition, spatial patters and environmental control on the Mediterranean Ridge mud volcanoes

Ritt B, Sarrazin J, Caprais J-C, Noël P, Gauthier O, Pierre C, Henry P, Desbruyères D (2010) First insights into the structure and environmental setting of cold-seep communities in the Marmara Sea. Deep Sea Research Part I: Oceanographic Research Papers 57: 1120-1136

Rouse GW, Fauchald K (1997) Cladistics and polychaetes. Zoologica Scripta 26: 139-204

Rouse GW, Pleijel F (2001) Polychaetes. Oxford University Press

Sahling H, Rickert D, Lee RW, Linke P, Suess E (2002) Macrofaunal community structure and sulfide flux at gas hydrate deposits from the Cascadia convergent margin, NE Pacific. Marine Ecology Progress Series 231:121-138

Salas C, Woodside J (2002) *Lucinoma kazani* n. sp. (Mollusca: Bivalvia): evidence of a living benthic community associated with a cold seep in the Eastern Mediterranean Sea. Deep Sea Research Part I: Oceanographic Research Papers 49: 991-1005

Sanders HL (1968) Marine benthic diversity: a comparative study. The American Naturalist 102: 243-282

Sarradin PM, Waeles M, Bernagout S, Le Gall C, Sarrazin J, Riso R (2009) Speciation of dissolved copper within an active hydrothermal edifice on the Lucky Strike vent field (MAR, 37° N). Science of the Total Environment 407: 869-878

Sarradin PM, Caprais JC (1996) Analysis of dissolved gases by headspace sampling gas chromatography with column and detector switching. Preliminary results. Analytical Communications 33: 371-373

Sarrazin J, Juniper SK (1999) Biological characteristics of a hydrothermal edifice mosaic community. Marine Ecology-Progress Series 185: 1-19

Shannon CE (1948) A mathematical theory of communication. Bell System Technical Journal 27: 379-423

Sibuet M, Olu K (1998) Biogeography, biodiversity and fluid dependence of deep-sea cold-seep communities at active and passive margins. Deep Sea Research Part II: Topical Studies in Oceanography 45: 517

Simpson EH (1949) Measurement of diversity. Nature 163: 688

Smith EB, Scott KM, Nix ER, Korte C, Fisher CR (2000) Growth and condition of seep mussels (Bathymodiolus childressi) at a Gulf of Mexico Brine Pool. Ecology 81: 2392-2403

Sommer S, Linke P, Pfannkuche O, Niemann H, Treude T (2009) Benthic respiration in a seep habitat dominated by dense beds of ampharetid polychaetes at the Hikurangi Maring (new Zealand). Marine Geology doi: 10.1016/j.margo.2009.06.003

Southward EC, Andersen AC, Hourdez S (in press) *Lamellibrachia anaximandri* n. sp., a new vestimentifera tubeworm from the Mediterranean (Annelida). Zoosystema

1089     Thistle D (2003) The deep-sea floor: an overview Ecosystems Of The Deep Ocean.
1090          Elsevier Science Bv, pp 5-37
1091     Tothmérész B (1998) On the characterization of scale-dependant diversity. Abstracta
1092          Bonatica 22: 149-156
1093     Treude T, Smith CR, Wenzhöfer F, Carney E, Bernardino AF, Hannides AK, Krüger
1094          M, Boetius A (2009) Biogeochemistry of a deep-sea whale-fall: sulfate
1095          reduction, sulfide efflux and methanogenesis. Marine Ecology Progess Series
1096          382: 1-21
1097     Van Gaever S, Moodley L, de Beer D, Vanreusel A (2006) Meiobenthos at the Arctic
1098          Håkon Mosby Mud Volcano, with a parental-caring nematode thriving in
1099          sulphide-rich sediments. Marine Ecology-Progress Series 321: 143-155
1100     Werne JP, Haese RR, Zitter T, Aloisi G, Bouloubassi I, Heijs S, Fiala-Medioni A,
1101          Pancost RD, Sinninghe Damste JS, de Lange G (2004) Life at cold seeps: a
1102          synthesis of biogeochemical and ecological data from Kazan mud volcano,
1103          eastern Mediterranean Sea. Chemical Geology 205: 367
1104     Whittaker RH (1960) Vegetation of the Siskiyou Mountains, Oregon and California.
1105          Ecological Monographs 30: 279
1106     Zitter TAC, Huguen C, Woodside JM (2005) Geology of mud volcanoes in the
1107          eastern Mediterranean from combined sidescan sonar and submersible
1108          surveys. Deep-Sea Research Part I-Oceanographic Research Papers 52: 457-
1109          475
1110     Zitter TAC, Woodside JM, Mascle J (2003) The Anaximander Mountains: a clue to
1111          the tectonics of southwest Anatolia. Geological Journal 38: 375-394

1112
1113
1114
1115
1116
1117
1118
1119
1120
1121
1122
1123
1124
1125
1126
1127
1128
1129
1130

**Table 1**. Location, depth, and tools used to perform physico-chemical and faunal sampling at each microhabitat from the different sampling sites of the Nile Deep-Sea Fan explored during the BIONIL (2006) and MEDECO (2007) cruises. Sampling effort, length of each sediment cores and estimated surface of each piece of carbonate crusts are also reported. Further details of samples are archived in http://www.pangaea.de/PHP/CruiseReports.php?b=HERMES

| Microhabitat types | Latitude (°N) | Longitude (°E) | Depth (m) | Physico-chemical measurements | Faunal sampling |
|---|---|---|---|---|---|
| **Reference site [ca. 15 km away from Amon MV (BIONIL, 2006)]** | | | | | |
| Reference site (Ref) | 32°21.42' | 31°32.50' | 1000 | 3 tubes (multicorer) M70/2b_785 | 3 tubes (74 cm² each) Ref1 (20 cm) Ref2 (20 cm) Ref3 (20 cm) |
| **Eastern Province – Amon MV (BIONIL, 2006)** | | | | | |
| Reduced sediments (Red) | 32°22.05' | 31°42.27' | 1154 | Microsensor , chamber and porewater samples PC15, 46, 47 M70/2b_765 (D115) M70/2b _790 (D121) | 3 blade cores (200 cm² each) Red1 (BCROV-2, 10 cm) Red2 (BCROV-3, 10 cm) Red3 (BCROV-8, 10 cm) |
| Carbonate crusts (CC) | 32°22.05' | 31°42.27' | 1153 | None | 3 pieces of crust CC1 (SFS-11, 84 cm²) CC2 (SFS-111, 103 cm²) CC3 (SFS-2, 139 cm²) |
| **Central Province – Pockmark area, site 2A (BIONIL 2006)** | | | | | |
| Reduced sediments (Red) | 32°32.01' | 30°21.13' | 1697 | Microsensor, chamber and porewater samples PC9, 52 M70/2b _784 (D120) M70/2b _841 (D127) | 3 blade cores (200 cm² each) Red1 (BCROV-3, 20 cm) Red2 (BCROV-7, 17 cm) Red3 (BCROV-8, 20 cm) |
| Carbonate crusts (CC) | 32°32.00' | 30°21.18' | 1696 | None | 3 pieces of crust CC1 (SFS-5, 48 cm²) CC2 (SFS-7, 81 cm²) CC3 (SFS-8, 34 cm²) |
| **Western Province – Cheops MV (MEDECO, 2007)** | | | | | |
| Reduced sediments (Red) | 32°08.05' | 28°09.67' | 3007 | 3x2 water samples: $CH_4$ MEDECO2_D343-PEPITO A-1 and PEPITO A-2, A-2, B-1, B-2, C-1 and C-2 | 3 blade cores (200 cm² each) Red1 (BL-2, 20 cm) Red2 (BL-4, 19 cm) Red3 (BL-6, 17 cm) |

**Table 2.** Physico-chemical characterization of the bottom water environment at the three study areas. Only the methane data from the Cheops MV were obtained directly above the organisms in this study. Amon data were provided by Girnth et al. (2011), Pockmark data by Grünke et al. (in press). $\Sigma S$ = Total dissolved sulphides ($H_2S+HS^-+S^{2-}$),  SR = Sulphate reduction rate. The reference site was ca. 15 km away from the active centre of the Amon MV.

| | pH | [O$_2$] Bottom water (µmol l$^{-1}$) | [O$_2$] Penetration depth (cm) | [O$_2$] Total benthic consumption (mmol m$^{-2}$ d$^{-1}$) | [SO$_4^{2-}$] Porewater (mmol l$^{-1}$) | [Cl$^-$] Porewater (mmol l$^{-1}$) | [CH$_4$] Bottom water (µmol l$^{-1}$) | [$\Sigma$S] Porewater (mmol l$^{-1}$) | [$\Sigma$S] Porewater top 5 cm/peak conc. (mmol l$^{-1}$) | SR Sediments (mmol m$^{-2}$ d$^{-1}$) |
|---|---|---|---|---|---|---|---|---|---|---|
| **Amon MV** | | | | | | | | | | |
| Reference site (Ref) | 8.20 [a] | 230 [a] | >4 [a] | < 1 [a] | 31.4 [a] | 529 [a] | 0.0 [a] | 0 [a] | - | < 0.2 [a] |
| Reduced sediments (Red) | 7.88 [b] | 150-200 [b] | 0.0-0.25 [b] | 10-46 [c] | 30.7-40.3 [d] | 404-580 [d] | 0.0 [d] | < 0.7 [b] | 0.8/2.5 [d] | 0.5 ± 0.2 (n=3) [d] |
| **Pockmark area** | | | | | | | | | | |
| Reduced sediments (Red) | 8.11 [b] | 230 [e] | 0.1-0.2 [b] | 156-174 [c] | 29.1-29.8 [d] | 606-630 [d] | 0.2-0.3 [e] | 0.2 [b] 0.7 [d] | 0.8/25 [d] | 22-41 [d] |
| **Cheops MV** | | | | | | | | | | |
| Reduced sediments (Red) | - | 220 [e] | - | 111-130 [c] | - | - | 3.60-9.34 [f] | - | - | 5-14 [d] |

Devices used to acquire the data: (a) multicorer, (b) microprofiler, (c) benthic chamber, (d) PCs, (e) KIPS bottle, (f) PEPITO, (-) no available data

**Table 3**. AMON - Macrofaunal (>250 μm) densities (individuals m$^{-2}$) per replicate and relative abundance (%) of each taxa in the microhabitats studied on the Amon mud volcano: reduced sediments (Red, n=3), carbonate crusts (CC, n=3) and the reference site (Ref, n=3). Total densities and relative abundances from each taxonomic group are highlighted in bold. Und. = undetermined individuals. (*) Taxonomic level used for alpha-diversity analyses, here mostly family level. All sampling was performed during the BIONIL cruise (2006).

| Taxonomic groups | Reduced sediments | | | | Carbonate crusts | | | | Reference samples | | | |
|---|---|---|---|---|---|---|---|---|---|---|---|---|
| | Red1 | Red2 | Red3 | % | CC1 | CC2 | CC3 | % | Ref1 | Ref2 | Ref3 | % |
| **Cnidaria (Total)** | **0** | **0** | **0** | **0** | **0** | **0** | **935** | **72.21** | **0** | **270** | **135** | **17.65** |
| Anthozoa – Zoantharia* | 0 | 0 | 0 | 0 | 0 | 0 | 935 | 72.21 | 0 | 0 | 0 | 0 |
| Medusozoa – Scyphozoa* | 0 | 0 | 0 | 0 | 0 | 0 | 0 | 0 | 0 | 270 | 135 | 17.65 |
| **Polychaeta (Total)** | **1900** | **400** | **1650** | **82.29** | **119** | **0** | **144** | **16.67** | **541** | **405** | **676** | **70.59** |
| Capitellidae* | 1100 | 100 | 50 | 26.04 | 0 | 0 | 0 | 0 | 0 | 0 | 0 | 0 |
| Dorvilleidae* | 300 | 50 | 1250 | 33.33 | 0 | 0 | 0 | 0 | 135 | 135 | 0 | 11.76 |
| Hesionidae* | 0 | 0 | 50 | 1.04 | 0 | 0 | 0 | 0 | 0 | 0 | 0 | 0 |
| Paraonidae* | 0 | 0 | 0 | 0 | 0 | 0 | 0 | 0 | 135 | 0 | 0 | 5.88 |
| Pholoidae* | 0 | 0 | 0 | 0 | 0 | 0 | 144 | 11.11 | 0 | 0 | 0 | 0 |
| Phyllodocidae* | 100 | 0 | 0 | 2.08 | 0 | 0 | 0 | 0 | 0 | 0 | 0 | 0 |
| Spionidae* | 100 | 0 | 50 | 3.13 | 0 | 0 | 0 | 0 | 135 | 135 | 405 | 29.41 |
| Siboglinidae, Frenulata* | 300 | 50 | 200 | 11.46 | 0 | 0 | 0 | 0 | 0 | 0 | 0 | 0 |
| Syllidae* | 0 | 0 | 0 | 0 | 119 | 0 | 0 | 5.56 | 0 | 0 | 270 | 11.76 |
| Terebellida* | 0 | 150 | 50 | 4.17 | 0 | 0 | 0 | 0 | 135 | 135 | 0 | 11.76 |
| Larvae | 0 | 50 | 0 | 1.04 | 0 | 0 | 0 | 0 | 0 | 0 | 0 | 0 |
| **Bivalvia (Total)** | **100** | **150** | **300** | **11.46** | **0** | **0** | **0** | **0** | **0** | **0** | **0** | **0** |
| Lucinidae* | | | | | | | | | | | | |
| *Lucinoma kazani* | 0 | 150 | 50 | 4.17 | 0 | 0 | 0 | 0 | 0 | 0 | 0 | 0 |
| Mytilidae* | | | | | | | | | | | | |
| *Idas modiolaeformis* | 50 | 0 | 0 | 1.04 | 0 | 0 | 0 | 0 | 0 | 0 | 0 | 0 |
| Thyasiridae* | | | | | | | | | | | | |
| *Thyasira striata* | 0 | 0 | 100 | 2.08 | 0 | 0 | 0 | 0 | 0 | 0 | 0 | 0 |
| Vesicomyidae* | | | | | | | | | | | | |
| *Isorropodon perplexum* | 0 | 0 | 150 | 3.13 | 0 | 0 | 0 | 0 | 0 | 0 | 0 | 0 |
| Sareptidae* | | | | | | | | | | | | |
| Und. Sareptidae | 50 | 0 | 0 | 1.04 | 0 | 0 | 0 | 0 | 0 | 0 | 0 | 0 |
| **Gastropoda (Total)** | **0** | **50** | **0** | **1.04** | **0** | **0** | **72** | **5.56** | **0** | **0** | **0** | **0** |
| Calliotropidae* | | | | | | | | | | | | |
| *Putzeysia wiseri* | 0 | 0 | 0 | 0 | 0 | 0 | 72 | 5.56 | 0 | 0 | 0 | 0 |
| Und. Gastropoda* | 0 | 50 | 0 | 1.04 | 0 | 0 | 0 | 0 | 0 | 0 | 0 | 0 |
| **Sipuncula (Total)** | **0** | **0** | **0** | **0** | **0** | **97** | **0** | **5.56** | **0** | **0** | **135** | **5.88** |
| Phascolosomatidae* | | | | | | | | | | | | |
| *Phascolosoma aff. granulatum* | 0 | 0 | 0 | 0 | 0 | 97 | 0 | 5.56 | 0 | 0 | 0 | 0 |
| Golfingiidae* | | | | | | | | | | | | |
| *Nephasoma minutum* | 0 | 0 | 0 | 0 | 0 | 0 | 0 | 0 | 0 | 0 | 135 | 5.88 |
| **Crustacea (Total)** | **50** | **50** | **150** | **5.21** | **0** | **0** | **0** | **0** | **0** | **0** | **135** | **5.88** |
| Decapoda-Thalassinidae* | 0 | 0 | 50 | 1.04 | 0 | 0 | 0 | 0 | 0 | 0 | 0 | 0 |
| Cumacea- Nannastacidae* | | | | | | | | | | | | |
| *Cumella pygmaea* | 0 | 0 | 50 | 1.04 | 0 | 0 | 0 | 0 | 0 | 0 | 0 | 0 |
| Isopoda* | 0 | 0 | 0 | 0 | 0 | 0 | 0 | 0 | 0 | 0 | 135 | 5.88 |
| Leptostraca* | 50 | 0 | 0 | 1.04 | 0 | 0 | 0 | 0 | 0 | 0 | 0 | 0 |

| Larvae | 0 | 50 | 50 | 2.09 | 0 | 0 | 0 | 0 | 0 | 0 | 0 | 0 |
|---|---|---|---|---|---|---|---|---|---|---|---|---|
| **Total densitiy (ind. m$^{-2}$)** | **2050** | **650** | **2100** | | **119** | **97** | **1151** | | **541** | **676** | **1081** | |

2
3
4
5
6
7
8
9
10
11
12
13
14
15
16
17
18
19
20
21
22
23
24
25
26
27
28
29
30
31
32
33
34
35
36
37
38
39
40
41
42
43
44
45
46
47
48
49
50
51
52
53
54
55
56
57
58

39

**Table 4**. POCKMARK area and CHEOPS - Macrofaunal (>250 µm) densities (individuals m$^{-2}$) per replicate and relative abundance (%) of each taxa in the microhabitats studied in the Pockmark area: reduced sediments (Red, n=3), carbonate crusts (CC, n=3) and on the Cheops MV: reduced sediments (Red, n=3). Total densities and relative abundances from each taxonomic group are highlighted in bold. Und. = undetermined individuals. (*) Taxonomic level used for alpha-diversity analyses, here mostly family level. All sampling was performed during the BIONIL (2006) and MEDECO (2007) cruises.

| Taxonomic groups | Pockmark area | | | | | | | | Cheops MV | | | |
| --- | --- | --- | --- | --- | --- | --- | --- | --- | --- | --- | --- | --- |
| | Reduced sediments | | | | Carbonate crusts | | | | Reduced sediments | | | |
| | Red1 | Red2 | Red3 | % | CC1 | CC2 | CC3 | % | Red1 | Red2 | Red3 | % |
| **Polychaeta (Total)** | **2550** | **2650** | **1800** | **83.83** | **1042** | **123** | **4412** | **39.62** | **3800** | **5100** | **3000** | **95.58** |
| Capitellidae* | 450 | 650 | 250 | 16.16 | 208 | 0 | 0 | 1.89 | 0 | 0 | 0 | 0 |
| Cirratulidae* | 0 | 0 | 0 | 0 | 208 | 0 | 0 | 1.89 | 0 | 0 | 0 | 0 |
| Dorvilleidae* | 1350 | 1500 | 1350 | 50.30 | 208 | 0 | 0 | 1.89 | 0 | 0 | 50 | 0.40 |
| Glyceridae* | 50 | 0 | 0 | 0.60 | 0 | 0 | 0 | 0 | 0 | 0 | 0 | 0 |
| Hesionidae* | 500 | 350 | 200 | 12.57 | 417 | 0 | 588 | 7.55 | 950 | 1050 | 1050 | 24.50 |
| Sabellidae* | 0 | 0 | 0 | 0 | 0 | 0 | 2941 | 18.87 | 0 | 0 | 0 | 0 |
| Spionidae* | 100 | 100 | 0 | 2.40 | 0 | 123 | 0 | 1.89 | 2750 | 2750 | 1300 | 54.62 |
| Syllidae* | 0 | 0 | 0 | 0 | 0 | 0 | 294 | 1.89 | 0 | 0 | 0 | 0 |
| Terebellida* | 100 | 50 | 0 | 1.80 | 0 | 0 | 588 | 3.77 | 100 | 1300 | 600 | 16.06 |
| **Bivalvia (Total)** | **350** | **500** | **50** | **10.78** | **0** | **0** | **1176** | **7.55** | **0** | **0** | **0** | **0** |
| Lucinidae* | | | | | | | | | | | | |
| *Lucinoma kazani* | 0 | 100 | 0 | 1.20 | 0 | 0 | 0 | 0 | 0 | 0 | 0 | 0 |
| Und. Lucinidae | 0 | 100 | 0 | 1.20 | 0 | 0 | 0 | 0 | 0 | 0 | 0 | 0 |
| Mytilidae* | | | | | | | | | | | | |
| *Idas modiolaeformis* | 0 | 0 | 0 | 0 | 0 | 0 | 1176 | 7.55 | 0 | 0 | 0 | 0 |
| Vesicomyidae* | | | | | | | | | | | | |
| *Isorropodon perplexum* | 100 | 150 | 0 | 2.99 | 0 | 0 | 0 | 0 | 0 | 0 | 0 | 0 |
| Und. Bivalvia | 150 | 150 | 50 | 5.39 | 0 | 0 | 0 | 0 | 0 | 0 | 0 | 0 |
| **Gastropoda (Total)** | **0** | **350** | **100** | **5.39** | **1667** | **1728** | **1471** | **50.94** | **0** | **50** | **50** | **0.80** |
| Calliotropidae* | | | | | | | | | | | | |
| *Putzeysia wiseri* | 0 | 0 | 0 | 0 | 208 | 123 | 294 | 5.66 | 0 | 0 | 0 | 0 |
| Trochidae* | 0 | 0 | 0 | 0 | 208 | 123 | 588 | 7.54 | 0 | 0 | 0 | 0 |
| Skeneidae* | | | | | | | | | | | | |
| *Akritogyra conspicua* | 0 | 0 | 0 | 0 | 0 | 123 | 0 | 1.9 | 0 | 0 | 0 | 0 |
| Und. *Skeneidae* | 0 | 100 | 0 | 1.20 | 0 | 0 | 0 | 0 | 0 | 0 | 0 | 0 |
| Orbitestellidae* | | | | | | | | | | | | |
| *Lurifax vitreus* | 0 | 0 | 0 | 0 | 1250 | 1358 | 588 | 35.85 | 0 | 0 | 0 | 0 |
| Und. Gastropoda | 0 | 250 | 100 | 4.19 | 0 | 0 | 0 | 0 | 0 | 50 | 50 | 0.80 |
| **Crustacea (Total)** | **0** | **0** | **0** | **0** | **0** | **0** | **294** | **1.89** | **200** | **100** | **150** | **3.61** |
| Amphipoda-Gammaridae | | | | | | | | | | | | |
| Sebidae* | | | | | | | | | | | | |
| *Seba sp.* | 0 | 0 | 0 | 0 | 0 | 0 | 294 | 1.89 | 0 | 0 | 0 | 0 |
| Und. Gammaridae | 0 | 0 | 0 | 0 | 0 | 0 | 0 | 0 | 50 | 0 | 0 | 0.40 |
| Leptostraca | | | | | | | | | | | | |
| Nebaliidae* | 0 | 0 | 0 | 0 | 0 | 0 | 0 | 0 | 0 | 0 | 50 | 0.40 |
| Und. Leptostraca | 0 | 0 | 0 | 0 | 0 | 0 | 0 | 0 | 150 | 100 | 100 | 2.81 |
| **Total density (ind. m$^{-2}$)** | **2900** | **3500** | **1950** | | **2708** | **1852** | **7353** | | **4000** | **5250** | **3200** | |

59
60

**Table 5**. AMON - Meiofaunal (>250 µm) densities (individuals m$^{-2}$) per replicate and relative abundance (%) of each taxa in the reduced sediment microhabitat (Red, n=3) studied on the Amon and in the reference samples (Ref, n=3). Total densities and relative abundances from each taxonomic group are highlighted in bold. Und. = undetermined individuals. (*) Taxonomic level used for alpha-diversity analyses, here mostly family level. All sampling was performed during the BIONIL cruise (2006).

| Taxonomic groups | Reduced sediments | | | | Carbonate crusts | | | | Reference site | | | |
|---|---|---|---|---|---|---|---|---|---|---|---|---|
| | Red1 | Red2 | Red3 | % | CC1 | CC2 | CC3 | % | Ref1 | Ref2 | Ref3 | % |
| **Nematoda (Total)** | **74650** | **29900** | **28300** | **95.15** | **0** | **388** | **0** | **100** | **405** | **135** | **405** | **77.78** |
| **Crustacea (Total)** | **900** | **1900** | **4000** | **4.85** | **0** | **0** | **0** | **0** | **270** | **0** | **0** | **22.22** |
| **Copepoda-Harpacticoida** | | | | | | | | | | | | |
| Miraciidae* | | | | | | | | | | | | |
| *Bulbamphiascus imus* | 500 | 1050 | 200 | 1.24 | 0 | 0 | 0 | 0 | 0 | 0 | 0 | 0 |
| *Bulbamphiascus* sp.1 | 0 | 0 | 0 | 0 | 0 | 0 | 0 | 0 | 0 | 0 | 0 | 0 |
| *Thyphlamphiascus confusus* | 0 | 0 | 550 | 0.39 | 0 | 0 | 0 | 0 | 0 | 0 | 0 | 0 |
| Ameiridae* | | | | | | | | | | | | |
| *Amphiascus* sp.2 | 0 | 0 | 0 | 0 | 0 | 0 | 0 | 0 | 0 | 0 | 0 | 0 |
| *Haifameira archibenthoica* | 0 | 400 | 2400 | 2.00 | 0 | 0 | 0 | 0 | 0 | 0 | 0 | 0 |
| *Haifameira* sp.1 | 0 | 0 | 200 | 0.14 | | | | | 0 | 0 | 0 | 0 |
| Agestidae* | | | | | | | | | | | | |
| *Eurycletodes sp.* | 0 | 0 | 0 | 0 | 0 | 0 | 0 | 0 | 270 | 0 | 0 | 22.22 |
| Tisbidae* | | | | | | | | | | | | |
| *Tisbella* sp. | 0 | 0 | 0 | 0 | 0 | 0 | 0 | 0 | 0 | 0 | 0 | 0 |
| Und. Harpacticoida | 0 | 0 | 50 | 0.07 | 0 | 0 | 0 | 0 | 0 | 0 | 0 | 0 |
| **Copepoda-Cyclopoida** | | | | | | | | | | | | |
| Oncaeidae* | | | | | | | | | | | | |
| *Oncaea* sp. | 0 | 0 | 50 | 0.04 | 0 | 0 | 0 | 0 | 0 | 0 | 0 | 0 |
| **Copepoda-Calanoida*** | | | | | | | | | | | | |
| *Calanoida* sp.1 | 0 | 150 | 450 | 0.43 | 0 | 0 | 0 | 0 | 0 | 0 | 0 | 0 |
| *Calanoida* sp. | 0 | 300 | 0 | 0.21 | 0 | 0 | 0 | 0 | 0 | 0 | 0 | 0 |
| Und. Calanoida | 300 | 0 | 0 | 0.21 | 0 | 0 | 0 | 0 | 0 | 0 | 0 | 0 |
| **Ostracoda** | | | | | | | | | | | | |
| Polycopidae* | | | | | | | | | | | | |
| *Polycope* sp.3M | 50 | 0 | 0 | 0.04 | 0 | 0 | 0 | 0 | 0 | 0 | 0 | 0 |
| Pontocyprididae* | | | | | | | | | | | | |
| *Propontocypris* sp.2M | 0 | 0 | 1 | 0.04 | 0 | 0 | 0 | 0 | 0 | 0 | 0 | 0 |
| *Propontocypris* cf. *levis* | 50 | 0 | 0 | 0.04 | 0 | 0 | 0 | 0 | 0 | 0 | 0 | 0 |
| % Meiofauna / Total fauna | **97.36** | **98.30** | **93.71** | | **0** | **80.00** | **0** | | **55.56** | **16.67** | **27.27** | |
| **Total density (ind. m$^{-2}$)** | **75500** | **31800** | **32300** | | **0** | **388** | **0** | | **676** | **135** | **405** | |

61
62
63
64
65
66
67
68
69
70
71
72
73

**Table 6**. POCKMARK area and CHEOPS – Meiofaunal (>250 μm) densities (individuals m$^{-2}$) per replicate and relative abundance (%) of each taxa in the microhabitats studied on the Pockmark area: reduced sediments (Red, n=3), carbonate crusts (CC, n=3) and on the Cheops mud volcano (MV): reduced sediments (Red, n=3). Total densities and relative abundances from each taxonomic group are given in bold. Und. = undetermined individuals. (*) Taxonomic level used for alpha-diversity analyses, here mostly family level. All sampling was performed during the BIONIL (2006) and MEDECO (2007) cruises.

| Taxonomic groups | Pockmark area | | | | | | | | Cheops MV | | | |
| --- | --- | --- | --- | --- | --- | --- | --- | --- | --- | --- | --- | --- |
| | Reduced sediments | | | | Carbonate crusts | | | | Reduced sediments | | | |
| | Red1 | Red2 | Red3 | % | CC1 | CC2 | CC3 | % | Red1 | Red2 | Red3 | % |
| **Nematoda (Total)** | **1100** | **500** | **1000** | **36.11** | **5417** | **247** | **2941** | **97.44** | **750** | **2850** | **600** | **100** |
| **Crustacea (Total)** | **2850** | **1300** | **450** | **63.89** | **0** | **123** | **0** | **2.56** | **0** | **0** | **0** | **0** |
| **Copepoda-Harpacticoida** | | | | | | | | | | | | |
| Miraciidae* | | | | | | | | | | | | |
| *Bulbamphiascus imus* | 1450 | 850 | 350 | 36.81 | 0 | 0 | 0 | 0 | 0 | 0 | 0 | 0 |
| Ameiridae* | | | | | | | | | | | | |
| *Amphiascus sp.2* | 0 | 0 | 0 | 0 | 0 | 123 | 0 | 2.56 | 0 | 0 | 0 | 0 |
| Tisbidae* | | | | | | | | | | | | |
| *Tisbella* sp. | 50 | 0 | 0 | 0.69 | 0 | 0 | 0 | 0 | 0 | 0 | 0 | 0 |
| **Copepoda-Cyclopoida** | | | | | | | | | | | | |
| *Cyclopina sp.* | 0 | 250 | 0 | 3.47 | | | | | | | | |
| **Copepoda-Calaonida*** | | | | | | | | | | | | |
| *Calanoida* sp.1 | 100 | 0 | 0 | 1.39 | 0 | 0 | 0 | 0 | 0 | 0 | 0 | 0 |
| *Calaonida* sp.2 | 50 | 0 | 0 | 0.69 | 0 | 0 | 0 | 0 | 0 | 0 | 0 | 0 |
| *Calaonida* sp.3 | 50 | 0 | 0 | 0.69 | 0 | 0 | 0 | 0 | 0 | 0 | 0 | 0 |
| *Calanoida* sp. | 250 | 0 | 0 | 3.47 | 0 | 0 | 0 | 0 | 0 | 0 | 0 | 0 |
| **Ostracoda** | | | | | | | | | | | | |
| Pontocyprididae* | | | | | | | | | | | | |
| *Propontocypris* sp.1M | 50 | 0 | 0 | 0.69 | 0 | 0 | 0 | 0 | 0 | 0 | 0 | 0 |
| *Propontocypris* cf.*levis* | 700 | 200 | 100 | 13.89 | 0 | 0 | 0 | 0 | 0 | 0 | 0 | 0 |
| *Propontocypris* cf. *setosa* | 50 | 0 | 0 | 0.69 | 0 | 0 | 0 | 0 | 0 | 0 | 0 | 0 |
| *Argilloecia* sp. | 50 | 0 | 0 | 0.69 | 0 | 0 | 0 | 0 | 0 | 0 | 0 | 0 |
| **Chelicerata** | | | | | | | | | | | | |
| Und. Acarina* | 50 | 0 | 0 | 0.69 | 0 | 0 | 0 | 0 | 0 | 0 | 0 | 0 |
| % Meiofauna / Total fauna | 57.66 | 33.96 | 42.65 | | 66.67 | 16.67 | 28.57 | | 15.79 | 35.19 | 15.79 | |
| **Total density (ind. m$^{-2}$)** | **3950** | **1800** | **1450** | | **5417** | **370** | **2941** | | **750** | **2850** | **600** | |

74
75
76
77
78
79
80
81
82
83
84
85
86
87
88
89

**Table 7**. RED - Biological descriptors of the reduced sediment microhabitats sampled on the Amon MV, the Pockmark area and the Cheops MV in the Nile Deep-Sea Fan. The highest values are highlighted in bold. The meiofaunal data includes only the large meiofauna >250 µm. The number equivalent of Shannon and Simpson indices are given in italics

| Biological descriptors | Amon | Pockmark area | Cheops |
|---|---|---|---|
| Macrofauna -dominant | Polychaetes reaching 82.3% of total abundance (Dorvilleidae, Capitellidae) | Polychaetes reaching 83.8% of total abundance (Dorvilleidae) | Polychaetes, reaching 95.6% of total abundance (Spionidae, Hesionidae) |
| Macrofauna -others | Bivalves, crustaceans, gastropods | Bivalves, gastropods | Crustaceans, gastropods |
| Mean macrofaunal densities (individuals m$^{-2}$) | 1 600 ± 912 | 2 783 ± 782 | **4 150 ± 1 033** |
| Mean Jaccard's similarity | 0.32 | 0.47 | **0.77** |
| Symbiont-bearing fauna | **17.1 – 36.4%** | 0 - 10% | 0% |
| Total macrofaunal biomass (kg preserved wet weight m$^{-2}$) | **1.2\*10$^{-1}$ ± 1\*10$^{-1}$** | 1.2\*10$^{-3}$ ± 1\*10$^{-3}$ | 6.4\*10$^{-3}$ ± 3\*10$^{-3}$ |
| **Macrofaunal diversity indices** | | | |
| Total richness (S) | **15** | 9 | 6 |
| Shannon (H$_e$') *Exp (H$_e$')* | **1.93** *6.89* | 1.35 *3.86* | 1.05 *2.86* |
| Gini-Simpson (D$_{GS}$) *(1 / 1-D$_{GS}$)* | **0.78** *4.62* | 0.63 *2.68* | 0.59 *2.44* |
| Evenness (J') | **0.71** | 0.61 | 0.59 |
| Meiofauna (>250µm) -dominant | Nematodes with 95.2% of the total abundance | Copepods with 63.9% of the total abundance | 100% nematodes |
| Meiofauna (>250µm) -others | Copepods, ostracods (6%) | Acarina (1.3%) | - |
| Mean meiofaunal densities (individuals m$^{-2}$) | **46 733 ± 25 004** | 2 400 ± 1 354 | 1 400 ± 1258 |
| Mean Jaccard's similarity | 0.31 | 0.41 | **0.67** |
| **Meiofaunal diversity indices** | | | |
| Total richness (S)* | **7** | **7** | 1 |
| Nematoda richmess | 1 | 1 | **1** |
| Copepoda richness | 4 | 3 | 0 |
| Ostracoda richness | 2 | 2 | 0 |
| Acarina richness | 0 | 1 | 0 |
| Shannon (H$_e$') *Exp (H$_e$')* | 0.24 *1.27* | **1.39** *4.01* | 0 |
| Gini-Simpson (D$_{GS}$) *(1 / 1-D$_{GS}$)* | 0.09 *1.10* | **0.70** *3.37* | - |
| Evenness (J') | 0.12 | **0.71** | - |

**Table 8**. CC and Ref - Biological descriptors of the carbonate crust microhabitats sampled on the Amon MV,in the Pockmark area and at the reference site (Amon MV) in the Nile Deep-Sea Fan. The highest values are highlighted in bold. The meiofauna data includes only the large meiofauna >250 µm. The number equivalent of Shannon and Simpson indices are given in italics

| Biological descriptors | Carbonate crusts | | Reference site |
|---|---|---|---|
| | Amon | Pockmark area | Amon |
| Macrofauna -dominant | Cnidarians (Zoantharia) reaching 72.2% of total abundance | Gastropoda (*Lurifax vitreus)* and polychaetes (Sabellidae) in various proportions, reaching 50.9, 39.6% of total abundance | Polychaetes, reaching a mean of 70.6% of total abundance (Spionidae) |
| Macrofauna -others | Gastropods, sipunculians | Bivalves, crustaceans | Cnidarians, sipunculians, crustaceans |
| Mean macrofaunal densities (individuals m$^{-2}$) | 456 ± 602 | **3 971 ± 2 960** | 766 ± 281 |
| Mean Jaccard's similarity | 0.0 | **0.31** | 0.34 |
| Symbiont-bearing fauna | 0% | 0 -**16**% | 0% |
| Total macrofaunal biomass (kg preserved wet weight m$^{-2}$) | 1.8*10$^{-3}$ ± 5*10$^{-2}$ | **3*10$^{-2}$ ± 5*10$^{-2}$** | 3.2*10$^{-5}$ ± 6*10$^{-5}$ |
| **Macrofaunal diversity indexes** | | | |
| Total richness (S) | 5 | **14** | 8 |
| Shannon (H$_e$') <br> *Exp (H$_e$')* | 0.96 <br> *2.61* | **2.08** <br> ***8.00*** | 1.92 <br> *6.82* |
| Gini-Simpson (D$_{GS}$ = 1- λ) <br> *(1 / λ )* | 0.46 <br> *1.84* | **0.81** <br> ***5.31*** | 0.83 <br> *5.90* |
| Evenness (J') | 0.60 | **0.79** | 0.92 |
| Meiofauna (>250µm) -dominant | Only 4 individuals (nematodes) | Nematodes with 97.4% of the total abundance | Only 9 individuals (nematodes, copepods) |
| Meiofauna (>250µm)-others | - | Copepods (11%) | - |
| Mean meiofaunal densities (individuals m$^{-2}$) | 129 ± 224 | **2 909 ± 2 523** | - |
| Mean Jaccard's similarity | - | 0.67 | - |
| **Meiofaunal diversity indexes** | | | |
| Total richness (S)* | 1 | 2 | 2 |
|     Nematoda richness | 1 | 1 | 1 |
|     Copepoda richness | 0 | 1 | 1 |
|     Ostracoda richness | 0 | 0 | 0 |
| Shannon (H$_e$') <br> *Exp (H$_e$')* | - | 0.12 <br> *1.13* | - |
| Gini-Simpson (D$_{GS}$ = 1- λ) <br> *(1 / λ )* | - | 0.05 <br> *1.05* | - |

| Evenness (J') | - | 0.17 | - |

90
91
92
93
94
95